Functional genomics reveals strain-specific genetic requirements conferring hypoxic growth in *Mycobacterium intracellulare*

Yoshitaka Tateishi[1,2*], Yuriko Ozeki[1], Akihito Nishiyama[1], Yuta Morishige[3], Yusuke Minato[4,5], Anthony D. Baughn[5], Sohkichi Matsumoto[1,6,7,8]

1. Department of Bacteriology, Graduate School of Medicine and Dental Sciences, Niigata University, 1-757, Asahimachi-dori, Chuo-ku, Niigata 951-8510, Japan.
2. Department of Microbiology, Fukushima Medical University, 1, Hikariga-oka, Fukushima City, Fukushima, 960-1295, Japan.
3. Department of Mycobacterium Reference and Research, Research Institute of Tuberculosis, Japan Anti-Tuberculosis Association, Kiyose, Tokyo, 2048533, Japan.
4. Department of Microbiology, Fujita Health University School of Medicine, Toyoake, Aichi, Japan.
5. Department of Microbiology and Immunology, University of Minnesota Medical School, 689 23rd Avenue S.E. Microbiology Research Facility, Minneapolis, 55455, MN, USA.
6. Laboratory of Tuberculosis, Institute of Tropical Disease, Universitas Airlangga,

19 Kampus C JI. Mulyorejo, Surabaya, 60113, Indonesia

20 7. Department of Bacteriology, Osaka Metropolitan University Graduate School of

21 Medicine, 1-4-3 Asahi-machi, Abeno-ku, Osaka 545-8586, Japan

22 8. Division of Research Aids, Hokkaido University Institute for Vaccine Research &

23 Development, Kita 20, Nishi 10, Kita-Ku, Sapporo, Hokkaido 001-0020, Japan

24 e-mail: y-tateishi@med.niigata-u.ac.jp, y-tate25@fmu.ac.jp

25

26 **Abstract**

27 *Mycobacterium intracellulare* is a major etiological agent of the recently expanding

28 *Mycobacterium avium–intracellulare* complex pulmonary disease (MAC-PD).

29 Therapeutic regimens that include a combination of macrolides and antituberculous

30 drugs have been implemented with limited success. To identify novel targets for drug

31 development that accommodate the genomic diversity of *M. avium–intracellulare*, we

32 subjected eight clinical MAC-PD isolates and the type strain ATCC13950 to genome-

33 wide profiling to comprehensively identify universally essential functions by transposon

34 sequencing (TnSeq). Among these strains, we identified 131 shared essential or growth-

35 defect-associated genes by TnSeq. Unlike the type strain, the clinical strains showed

36 increased requirements for genes involved in gluconeogenesis and the type VII

37 secretion system under standard growth conditions, the same genes required for hypoxic
38 pellicle-type biofilm formation in ATCC13950. Consistent with the central role of
39 hypoxia in the evolution of *M. intracellulare*, the clinical MAC-PD strains showed more
40 rapid adaptation to hypoxic growth than the type strain. Importantly, the increased
41 requirements of hypoxic fitness genes were confirmed in a mouse lung infection model.
42 These findings confirm the concordant genetic requirements under hypoxic conditions
43 *in vitro* and hypoxia-related conditions *in vivo*, and highlight the importance of using
44 clinical strains and host-relevant growth conditions to identify high-value targets for
45 drug development.
46

47 **Introduction**

48 In contrast to the ongoing decline in the rate of tuberculosis, *Mycobacterium avium–*
49 *intracellulare* complex pulmonary disease (MAC-PD) is increasing in many parts of the
50 world[1,2]. The standard therapy for MAC-PD involves multidrug chemotherapy that
51 includes clarithromycin and several antituberculous drugs. Unfortunately, treatment
52 failure is common, resulting in relapse, disease progression, and death[3]. Therefore, it is
53 critical to investigate the bacterial physiological characteristics that underlie the ability
54 of MAC-PD strains to establish and maintain chronic drug-recalcitrant infections.

55 Recent advances in comparative genomics have revealed major differences in
56 the genomic features of reference type strains and circulating pathogenic clinical
57 isolates. Extensive genomic diversity has been recognized across clinical isolates of
58 nontuberculous mycobacteria (NTM). *Mycobacterium avium* has been divided into four
59 subspecies including subspecies, *avium*, *hominissuis*, *silvaticum*, and *paratuberculosis* [4].
60 Whereas *M. intracellulare* has been divided into two subgroups, typical *M.*
61 *intracellulare* (TMI) and *M. paraintracellulare–M. indicus pranii* (MP-MIP), with
62 currently two additional distinguished subspecies, *yongonense*, and *chimaera*[5,6]. Despite
63 the increasing number of sequenced MAC-PD strains, the molecular genetic
64 mechanisms that underlie their virulence and pathogenesis are still poorly understood.
65 The burgeoning field of functional genomics has allowed the rapid assessment
66 of molecular aspects of organisms on a genome-wide scale. Transposon (Tn) sequencing
67 (TnSeq) is a functional genomic approach that combines saturation-level transposon-
68 insertion mutagenesis with next-generation sequencing (NGS) to comprehensively
69 evaluate the fitness costs associated with gene inactivation in bacteria. Over the last
70 decade, TnSeq has been applied to numerous bacterial species using various
71 approaches[7]. Whereas initial studies applied TnSeq to reference strains, recent
72 approaches have included the comparative assessment of representative clinical strains

73 to better understand the fundamental aspects of pathogen biology[8,9]. We have previously
74 used TnSeq to globally characterize the genes that are essential for growth versus those
75 that are essential for hypoxic pellicle formation in the *M. intracellulare* type strain
76 ATCC13950[10]. However, given the recent expansion of MAC-PD and the well-
77 recognized high levels of genomic diversity in this complex of bacteria, data obtained
78 from the study of a decades-old reference strain is not expected to represent the
79 diversity of extant clinical isolates. ATCC13950 was originally isolated from the
80 abdominal lymph node of the 34-month-old female[11]. Even though the etiological
81 bacterial species are the same, the clinical manifestation of infant lymphadenitis differs
82 markedly from MAC-PD, which often occurs in middle-aged and elderly female
83 patients with no predisposing immunological disorder. So far, there are a total of two
84 reports on TnSeq that compare genetic requirements between clinical mycobacterial
85 strains and the type strains in *M. tuberculosis*[8] and *M. abscessus*[9]. They reported the
86 diversity of genetic requirements among strains including the type strain such as *M.*
87 *tuberculosis* H37Rv and *M. abscessus* ATCC19977. Therefore, it is essential to
88 investigate a collection of strains that captures the diversity of recent clinical MAC-PD
89 strains in order to define key molecular aspects of their pathogenesis and virulence.
90 In this study, we used TnSeq to analyze a set of recently isolated clinical *M.*

91 *intracellulare* strains with diverse genotypes. We integrated the gene essentiality data
92 for these strains and the type strain to identify the common essential and growth-defect-
93 associated genes that represent the genomic diversity of this group of pathogens. We
94 also identified the greater requirements of genes involved in gluconeogenesis, the type
95 VII secretion system, and cysteine desulfurase in the clinical MAC-PD strains than in
96 the type strain. Furthermore, the requirement for these genes was confirmed in a mouse
97 lung infection model. The profiles of genetic requirements in clinical MAC-PD strains
98 suggest the mechanism of hypoxic adaptation in NTM in terms of promising drug
99 targets, especially for strains that cause clinical MAC-PD.
100

101 **Results**

102 **Common essential and growth-defect-associated genes representing the genomic**
103 **diversity of *M. intracellulare* strains**

104 To obtain comprehensive information on the genome-wide gene essentiality of *M.*
105 *intracellulare*, we included nine representative strains of *M. intracellulare* with diverse
106 genotypes for TnSeq *in vitro* in this study (Fig. 1a, b, Supplementary Fig. 1,
107 Supplementary Table 1). We used TRANSIT[12] to obtain 2–6 million reads of Tn
108 insertions. The average number of Tn insertion reads was > 50 at Tn-inserted TA sites,

109 which confirmed the TnSeq data (Supplementary Table 2). The numbers of essential
110 genes in the clinical MAC-PD strains, calculated with the hidden Markov model
111 (HMM; a transition probability model), tended to be smaller than that in ATCC13950
112 (Supplementary Table 3). In total, 131 genes were identified as essential or growth-
113 defect-associated with the HMM analysis across all *M. intracellulare* strains, including
114 the eight MAC-PD clinical strains and ATCC13950 (Fig. 2a, Supplementary Table 4).
115 The genes identified as universal essential or growth-defect-associated were involved in
116 fundamental functions, such as glyoxylate metabolism, purine/pyrimidine metabolism,
117 amino acid synthesis, lipid biosynthesis, arabinogalactan/peptidoglycan biosynthesis,
118 porphyrin metabolism, DNA replication, transcription, amino acid tRNA ligases,
119 ribosomal proteins, general secretion proteins, components of iron–sulfur cluster
120 assembly, some ABC transporters, and the type VII secretion system. The genes
121 identified corresponded to the genes that encode conventional and under-development
122 drug targets, such as those encoding gyrase, arabinosyltransferase, enoyl-(acyl-carrier-
123 protein) reductase, alanine racemase, DNA-directed RNA polymerase, malate
124 synthase[13] and F_0F_1 ATP synthase (Fig. 2b). These data suggest that the set of universal
125 essential or growth-defect-associated genes identified with the HMM analysis of *M.*
126 *intracellulare* strains with diverse genotypes has potential utility as antibiotic drug

127 targets.

128

129 **The sharing of strain-dependent and accessory essential and growth-defect-**

130 **associated genes with genes required for hypoxic pellicle formation in the type**

131 **strain ATCC13950**

132 By comparative genomic analysis, we have revealed 3,153 core genes among

133 55 *M. intracellulare* strains including those used in this study[5] (Supplementary Fig. 1).

134 Of these core genes, 439 genes were classified as strain-dependent essential or growth-

135 defect-associated with the HMM analysis (Supplementary Table 5). And among 5,824

136 accessory genes, 222 genes were classified as essential or growth-defect-associated with

137 the HMM analysis. The proportion of these strain-dependent and accessory essential or

138 growth-defect-associated genes was comparable to the similar analysis of *Streptococcus*

139 *pneumoniae*[14]. Of note, 17 (3.8%) of strain-dependent essential or growth-defect-

140 associated genes and 14 (6.3%) of accessory essential or growth-defect-associated genes

141 were also included in the 175 genes required for hypoxic pellicle formation in

142 ATCC13950 reported in our previous study[10] (Supplementary Table 6). Gene set

143 enrichment analysis (GSEA)[15] showed that 9.1% (16 out of 175) genes were hit as core

144 enrichment (Supplementary Table 6). Of them, 4 genes were hit commonly as genes

145 showing increased genetic requirements analyzed by resampling plus HMM analyses
146 including genes of phosphoenolpyruvate carboxykinase *pckA* (OCU_RS48660), type
147 VII secretion-associated serine protease *mycP5* (OCU_RS38275), type VII secretion
148 protein eccC5 (OCU_RS38345) and glycine cleavage system amino-methyltransferase
149 *gcvT* (OCU_RS35955).
150

151 **Partial overlap of the genes showing increased genetic requirements in clinical**
152 **MAC-PD strains with those required for hypoxic pellicle formation in the type**
153 **strain ATCC13950**

154 The profiles of genetic requirements in each bacterial strain reflect the adaptation to
155 the environment in which each strain lives. When the strains are placed in a special
156 environment, they can adapt to the situation by altering the profiles of genetic
157 requirements, resulting in the remodeling of metabolic pathways. The sharing of strain-
158 dependent and accessory essential or growth-defect-associated genes with genes
159 required for hypoxic pellicle formation in ATCC13950 prompts us to consider that the
160 profiles of genetic requirements in clinical MAC-PD strains may be associated with the
161 genes required for hypoxic pellicle formation in ATCC13950. To clarify this, we
162 compared the genetic requirements of the clinical MAC-PD strains with that in

163 ATCC13950 by integrating the HMM analysis with the resampling analysis, a method
164 of calculating the number of significantly altered Tn insertion reads (a gene-based
165 permutation model). With this integrating analysis, 121 genes in the clinical MAC-PD
166 strains were shown to have significantly fewer Tn insertions than ATCC13950 (Fig. 3,
167 Supplementary Tables 7, 8). Of these, nine genes were identified in 3–5 clinical MAC-
168 PD strains. These included genes encoding phosphatases (OCU_RS30185,
169 OCU_RS35795), cysteine desulfurase (*csd* [OCU_RS40305]), methyl transferase
170 (OCU_RS41540), a hypothetical protein (OCU_RS47290), type VII secretion
171 components (*mycP5* [OCU_RS38275], *eccC5* [OCU_RS38345]), a glycine cleavage
172 system aminomethyltransferase (*gcvT* [OCU_RS35955]), and phosphoenolpyruvate
173 carboxykinase (*pckA* [OCU_RS48660]) (Figs 3, 4). The genes involved in
174 gluconeogenesis (such as *pckA*), the glycine cleavage system, and the type VII secretion
175 system were also identified as required for hypoxic pellicle formation in ATCC13950 in
176 our previous study[9]. The Tn insertion reads were significantly reduced in the pathways
177 of gluconeogenesis, including in fructose-1,6-bisphosphatase (*glpX*),
178 phosphoenolpyruvate carboxykinase (*pckA*), and pyruvate carboxylase (*pca*), but were
179 significantly increased in those of glycolysis, including in pyruvate kinase (*pykA*) and
180 pyruvate dehydrogenase (*aceE*, *lpdC*), suggesting that carbohydrate metabolism was

181 metabolically remodeled in the clinical MAC-PD strains, which mimics the metabolism

182 observed during hypoxic pellicle formation in ATCC13950 (Fig. 5).

183

184 **Minor role of gene duplication on reduced genetic requirements in clinical MAC-**

185 **PD strains**

186 On the other hand, 162 genes were detected with significantly more Tn insertions in

187 the clinical MAC-PD strains than in ATCC13950 (Fig. 3). Of these, 12 genes were

188 identified in more than seven strains. The increased Tn insertion reads in the genes

189 encoding superoxide dismutase (OCU_RS25945) and pyruvate dehydrogenase (*aceE*

190 [OCU_RS35720]) in the clinical MAC-PD strains suggest the inessentiality of the

191 detoxification of oxygen radicals and glycolysis metabolism in these strains (Figs 3–5).

192 These genes also included those encoding amidohydrolases (OCU_RS34400,

193 OCU_RS34425, OCU_RS34445), some transcription factors (OCU_RS28440,

194 OCU_RS30230), a CoA transferase (OCU_RS34390), and some predicted transporters

195 (OCU_RS28435, OCU_RS39950, OCU_RS39955, OCU_RS44685). Furthermore, the

196 increase in Tn insertion reads in predicted multidrug-resistant genes, such as those

197 encoding the DrrAB-ABC transporter complex (OCU_RS39950, OCU_RS39955)[16] and

198 a putative lipoprotein LpqB (OCU_RS44685), encoded by the two-component system

199 *mtrAB* operon[17-18], in the clinical MAC-PD strains were found.

200 In order to investigate the effect of gene duplication on the change of genetic
201 requirements between strains, we conducted blast search for the 162 genes showing
202 increased Tn insertion reads in the clinical MAC-PD strains compared to ATCC13950.
203 We found that M019 has duplicate genes of OCU_RS44705 coding
204 adenosylhomocysteinase (LOCUS_42940: ahcY_1, LOCUS_21000: ahcY_2).
205 However, there were no duplicate genes found in the remaining 161 genes. These data
206 suggest that gene duplication has minor effects on the change of genetic requirements
207 between strains. Rather, sequence differences and accessory genes may play a key role
208 in determining the difference of genetic requirements.

209

210 **Identification of genes in the clinical MAC-PD strains required for mouse lung**
211 **infection**

212 Hypoxia is the major environmental condition in natural water[19], biofilms[20], and
213 infections in humans and animals characterized by caseous granuloma lesions[21]. The
214 impact of hypoxia on mycobacteria under various ecological circumstances implies that
215 the genes required for pathogenesis of MAC-PD may be in some degrees, overlapped
216 with the genes with increased requirements in the clinical MAC-PD strains compared to

217 ATCC13950, and also with the genes required for hypoxic pellicle formation in
218 ATCC13950. To identify genes required for *in vivo* infection of clinical MAC-PD
219 strains, we performed TnSeq in mice infected intratracheally with the Tn mutant library
220 strains of M.i.198 or M.i.27, which we had demonstrated to be virulent in mice (Fig. 1b,
221 Supplementary Fig. 3)[22]. (It is impossible to perform TnSeq in mouse lungs infected
222 with ATCC13950 because ATCC13950 is eliminated within 4 weeks of infection[22].) The
223 time course of the changes in the bacterial burden showed a pattern similar to those of
224 the wild-type strains M.i.198 and M.i.27, respectively, except that it was not possible to
225 harvest sufficient colonies (as few as 10^4/mouse) in the few mice infected with the
226 M.i.27 Tn mutant strain in Week 8 and Week 16 (Supplementary Fig. 3b,
227 Supplementary Table 9). With a resampling analysis, 629 and 512 genes were shown to
228 be required for *in vivo* infection with transposon mutant library strains M.i.27 and
229 M.i.198, respectively, at least at one time point between Day 1 and Week 16 of infection
230 (Fig. 6a, Supplementary Fig. 3c, d, Supplementary Tables 10, 11). Of these genes, 72
231 (11.9%) and 50 (9.76%) in M.i.27 and M.i.198, respectively, were also required for
232 hypoxic pellicle formation in ATCC13950. Forty-one genes also required for hypoxic
233 pellicle formation in ATCC13950 were identified in both M.i.27 and M.i.198, and
234 included genes associated with succinate production (multifunctional 2-oxoglutarate

235 metabolism enzyme) and the glyoxylate cycle (isocitrate lyase), cysteine and
236 methionine synthesis (thiosulfate sulfurtransferase [CysA], 5-methyltetrahydrofolate-
237 homocysteine methyltransferase [MetH]), the serine/threonine-protein kinase PknG
238 system, proteasome subunits (PrcA, PrcB), DNA repair UvrC, secretion protein EspR,
239 cell-wall synthesis proteins (such as phosphatidylinositol [polyprenol-phosphate-
240 mannose-dependent alpha-[1-2]-phosphatidylinositol pentamannoside
241 mannosyltransferase], peptidoglycan (penicillin-binding protein A pbpA), and L,D-
242 transpeptidase 2), putative membrane proteins and transporters (such as the MmpL
243 family, transport accessory protein MmpS3, transport protein MmpL11, vitamin B_{12}
244 transport ATP-binding protein BacA, ABC transporter substrate-binding protein, and
245 ABC transporter permease), and mammalian cell entry (Mce) proteins
246 (OCU_RS48855–48875) (Supplementary Table 12).
247 At all timepoints from Day1 to Week 16, there were 74 and 99 genes were
248 shown to be required for lung infection with M.i.27 and M.i.198, respectively. Of them,
249 21 (28.3%) and 12 (12.1%) genes belonged to the genes involved in hypoxic pellicle
250 formation in the type strain. At timepoints throughout Week 4 to Week 16 except for
251 Day1, there were 121 and 172 genes were shown to be required for lung infection with
252 M.i.27 and M.i.198, respectively. Of them, 21 (23.1%) and 30 (18.0%) genes belonged

253 to genes involved in hypoxic pellicle formation in the type strain. These hypoxic
254 pellicle-associated genes detected both in M.i.27 and M.i.198 encoded methionine
255 synthesis (MetH), acyl-CoA dehydrogenase, isocitrate lyase, MMPL family transporter
256 (MmpL11) (from Day1 to Week 16), additionally multifunctional oxoglutarate
257 decarboxylase/dehydrogenase, proteasome subunits (PrcA, PrcB), ABC transporter
258 ATP-binding protein/permease, lipase chaperone (from Week 4 to Week 16) (new
259 Supplementary Tables 13, 14).

260 The genes only identified in M.i.27 that were also required for hypoxic pellicle
261 formation in ATCC13950 included genes associated with gluconeogenesis (*pckA*, *glpX*),
262 the glycine cleavage system (*gcvT*), the type VII secretion system (*eccD5, espG5,*
263 *eccC5* [OCU_RS38280-OCU_RS38285-OCU_RS38345], *eccC3* [OCU_RS48145]),
264 and D-inositol 3-phosphate glycosyltransferase (Supplementary Table 12). These three
265 systems, gluconeogenesis, the glycine cleavage system, and the type VII secretion
266 system, also showed increased genetic requirements in 3–5 clinical MAC-PD strains
267 than in ATCC13950 (Figs 3, 6). Although M.i.27 was excluded as a relevant strain
268 showing increased genetic requirements of these three metabolic systems, the increase
269 in genetic requirements for infection *in vivo* suggests a positive relationship between
270 hypoxic growth *in vitro* and bacterial growth *in vivo*. In contrast, M.i.198 already

271 showed increased genetic requirements in these three metabolic systems under aerobic
272 conditions *in vitro*, so the genes associated with these three systems were not identified
273 as having fewer Tn insertion reads during infection *in vivo*. Genes only identified in
274 M.i.198 and required for hypoxic pellicle formation in ATCC13950 included genes
275 associated with succinate synthesis (2-oxoglutarate oxidoreductase subunit KorA) or
276 encoding the HTH-type transcriptional repressor KstR and menaquinone reductase
277 (Supplementary Table 12). As increased genetic requirements in 3–5 clinical strains
278 (excluding M.i.198) compared with ATCC13950, an increased requirement for the RNA
279 methyltransferase OCU_RS41540 was identified in M.i.198 during infection *in vivo*.
280 These *in vivo* TnSeq data suggest that, despite the differences in the profiles of the
281 genes required for *in vivo* infection between strains, increase of genetic requirements for
282 hypoxic growth in part contribute to the pathogenesis *in vivo*.
283 We have performed a statistical enrichment analysis of gene sets by GSEA[15] to
284 investigate whether the genes required for growth of M.i.27 and M.i.198 in mouse lungs
285 overlap the gene sets required for hypoxic pellicle formation in ATCC13950 as well as
286 the gene sets showing increased genetic requirements observed in the clinical MAC-PD
287 strains listed in Fig 3. Of these gene sets including a total of 180 genes, 54% (98 genes)
288 and 40% (73 genes) were listed as enriched in genes required for mouse infection in

289 M.i.27 and M.i.198, respectively ($P < 0.01$ in M.i.27 and $P = 0.016$ in M.i.198)
290 (Supplementary Fig. 4, Supplementary Table 15). The enriched genes both in M.i.27
291 and M.i.198 included genes encoding fructose -1,6-bisphosphatase (*glpX*), a type VII
292 secretion protein (*eccC5*), glycine cleavage system aminomethyltransferase (*gcvT*),
293 some phosphatase (OCU_RS30185) and a hypothetical protein (OCU_RS47290) (Fig.
294 6). The enriched genes only in M.i.27 included genes of phosphoenolpyruvate
295 carboxylinase (*pckA*), cysteine desulfurase (*csd*) and the ESX-5 type VII secretion
296 component serine protease (*mycP5*). The enriched genes only in M.i.198 included genes
297 encoding some phosphatase (OCU_RS35975) and class I SAM-dependent RNA
298 methyltransferase (OCU_RS41540). Similarly, 40-50% of the genes required for
299 ATCC13950's hypoxic pellicle formation and strain-dependent/accessory essential
300 genes are significantly enriched individually with the genes required for *in vivo* bacterial
301 growth (Supplementary Figs. 5, 6, Supplementary Tables 16, 17). These data suggest the
302 sharing of the hypoxia-adaptation pathways between *in vitro* hypoxic pellicle formation
303 and *in vivo* bacterial growth.
304
305 **Effects of knockdown of universal essential or growth-defect-associate genes in**
306 **clinical MAC-PD strains**

307 To facilitate the functional analysis of the TnSeq-hit genes, it is necessary to construct
308 the genetically-engineered strains. Still now, there are very few reports of gene
309 engineering of MAC strains and none of them has been accompanied by the follow-up
310 studies[23-28]. Moreover, no attempts have been reported to construct the knockdown
311 strains in MAC strains. With an intention to evaluate the effect of suppressing TnSeq-hit
312 genes on bacterial growth, we used the pRH2052/pRH2521 clustered regularly
313 interspaced short palindromic repeats interference (CRISPR-i) plasmids to construct
314 knockdown strains where the expression of the target gene is suppressed[29-31]. Of the
315 nine *M. intracellulare* strains analyzed in this study, seven could be transformed with
316 the vectors for single guide RNA (sgRNA) expression and dCas9 expression. However,
317 the other two strains, M001 and MOTT64, could not be transformed with these
318 CRISPR-i vectors. To confirm the gene essentiality detected with the HMM analysis,
319 we evaluated the consequent growth inhibition in the knockdown strains of
320 representative universal essential or growth-defect-associated genes, including *glcB*,
321 *inhA*, *gyrB*, and *embB*. The knockdown strains showed growth suppression with
322 comparative growth rates of knockdown strains to vector control strains that do not
323 express single sgRNA reaching 10^{-1} to 10^{-4} (Fig. 7a).
324

325 **Differential effects of knockdown of accessory/strain-dependent essential or**

326 **growth-defect-associated genes among clinical MAC-PD strains**

327 As representative accessory and strain-dependent essential or growth-defect-

328 associated genes, we evaluated the 9 genes showing reduced Tn insertion reads in the 3–

329 5 clinical MAC-PD strains as listed in Fig. 3, as well as *glpX*, a gene of gluconeogenesis

330 where four MAC-PD strains showed reduced Tn insertion reads in a resampling analysis

331 (Fig. 5b). The growth was suppressed in the *pckA*-knockdown strains in M.i.198 and

332 M003, in the *glpX*-knockdown strain in M003, and in the cysteine desulfurase gene

333 (*csd*)-knockdown strains in M.i.198 and M003, with comparative growth rates of

334 knockdown strains to vector control strains reaching 10^{-2} to 10^{-4} (Fig. 7b). The growth

335 tended to be suppressed in the type VII secretion protein gene (*eccC5*)-knockdown

336 strain in M003 and in the type VII secretion-associated serine protease mycosin gene

337 (*mycP5*)-knockdown strain in M003, with comparative growth rates of knockdown

338 strains to vector control strains reaching less than 10^{-1}. By contrast, the growth was not

339 suppressed in these knockdown strains in ATCC13950, with comparative growth rates

340 of knockdown strains to vector control strains not reaching 10^{-1}, which was consistent to

341 the inessentiality of these genes under aerobic conditions in ATCC13950. As for

342 M.i.198 and M003, the consistency between TnSeq data and CRISPR-i data was

343 supported by a correlation between the growth suppression of the knockdown strains
344 and the fitness costs evaluated by a resampling analysis (Supplementary Table 18).
345 In contrast to the cases of M.i.198 and M003, the growth of knockdown strains
346 of the accessory and strain-dependent essential genes was not effectively suppressed in
347 the other MAC-PD strains despite being positively detected in TnSeq (Fig. 7b,
348 Supplementary Fig. 7). Although the gene expression levels were not suppressed to <
349 1% as reported in *M. tuberculosis* (Mtb)[32], the suppression of gene expression was
350 confirmed to approximately 20-70% in the knockdown strains of these accessory and
351 strain-dependent essential or growth-defect-associate genes, as well as universal
352 essential or growth-defect-associated genes such as *glcB*, *inhA*, *gyrB*, and *embB*
353 (Supplementary Fig. 8). The possible reason may be explained by the recently revealed
354 bypass mechanism of gene essentiality in strain-dependent/accessory essential or
355 growth-defect-associated genes, where gene essentiality can be bypassed by several
356 mechanisms including the composition of the accessory genome and pathway
357 rewiring[14].
358 To be summarized, we could validate the universal essential or growth-defect-
359 associated genes by the CRISPR-i system in the *M. intracellulare* strains used in this
360 study. And, although not successful with all strains, we could validate the accessory and

361 strain-dependent essential or growth-defect-associated genes, especially genes of
362 gluconeogenesis, type VII secretion components and iron-sulfur cluster assembly in
363 several MAC-PD strains like M.i.198 and M003.
364
365 **Preferential hypoxic adaptation of clinical MAC-PD strains evaluated with**
366 **bacterial growth kinetics**
367 The metabolic remodeling, such as the increased genetic requirements of
368 gluconeogenesis and the type VII secretion system, and the overlap of the genes
369 required for mouse lung infection and those required for hypoxic pellicle formation
370 involved by these metabolic pathways suggest the preferential adaptation of the clinical
371 MAC-PD strains to hypoxic conditions. To confirm this, we investigated the growth
372 kinetics of each strain under aerobic and hypoxic conditions. In terms of growth
373 kinetics, most of the clinical MAC-PD strains (except M001) entered logarithmic (log)
374 phase earlier than ATCC13950 under 5% oxygen (Fig. 8a, 8b, Supplementary Table 19).
375 However, under aerobic conditions, the clinical MAC-PD strains entered log phase at a
376 similar time to ATCC13950. The growth rate at mid-log point (midpoint) was
377 significantly reduced under hypoxic conditions in a total of 5 clinical MAC-PD strains
378 (M.i.198, M.i.27, M003, M019 and M021) compared to aerobic conditions (Fig. 8a, 8b,

379 Supplementary Table 19). The growth rate at midpoint under hypoxic conditions was
380 significantly lower in these 5 clinical MAC-PD strains than in ATCC13950. By contrast,
381 the growth rate at midpoint was significantly increased under hypoxic conditions
382 compared to aerobic conditions in ATCC13950. And there was no significant change in
383 the growth rate between aerobic and hypoxic conditions in the rest 3 clinical MAC-PD
384 strains (M018, M001 and MOTT64).
385
386 **The pattern of hypoxic adaptation not simply determined by genotypes**
387 Since ATCC13950 and M018 are phylogenetically neighbors within the same TMI
388 group each other, there may be a claim that the growth phenotypes of a longer lag phase
389 compared to other strains under hypoxic conditions might be determined simply by the
390 genotypes. To examine this, we performed hypoxic growth assay for additional two
391 strains (M005, M016) phylogenetically more closely related to ATCC13950
392 (Supplementary Fig. 1, Supplementary Table 1). The result showed different growth
393 pattern under hypoxia; M005 reached midpoint later than ATCC13950, by contrast
394 M016 reached midpoint three-quarters earlier than ATCC13950 (Supplementary Fig. 9).
395 These data suggest that genotypes seem to have some impact on bacterial growth
396 pattern under hypoxia; however, since there was a significant difference in the timing of

397 hypoxic adaptation among ATCC13950 and its neighbor strains, bacterial growth
398 pattern under hypoxia seems to be determined by multiple factors other than genotypes
399 such as strain-specific profiles of genetic requirements and unproven regulatory
400 systems.

401 In summary, the data of more rapid adaptation to hypoxia followed by reduced
402 growth rate once adapted indicate the greater metabolic advantage on continuous
403 logarithmic bacterial growth under hypoxic conditions in the clinical MAC-PD strains
404 than in ATCC13950. Because the profiles of genetic requirements reflect the adaptation
405 to the environment in which bacteria habits, it is reasonable to assume that the increase
406 of genetic requirements in hypoxia-related genes such as gluconeogenesis (*pckA, glpX*),
407 type VII secretion system (*mycP5, eccC5*) and cysteine desulfurase (*csd*) play an
408 important role on the growth under hypoxia-relevant conditions *in vivo*.

409

410 **Discussion**

411 In this study, using TnSeq of nine genetically diverse *M. intracellulare* strains, we have
412 identified 131 shared essential and growth-defect-associated genes with an HMM
413 analysis. The genes identified are promising drug targets, representing the genomic
414 diversity of the clinical MAC-PD strains and reflecting the actual clinical situation. The

415 strategy of narrowing the essential genes of bacteria is a useful approach for refining the
416 database of drug targets. We have also demonstrated an overview of the differences in
417 genetic requirements for hypoxic growth between the ATCC type strain and the clinical
418 *M. intracellulare* strains responsible for MAC-PD, with the evidence of earlier entry to
419 log phase followed by slower growth rate observed in most of these clinical strains
420 compared to ATCC13950. This is the first study to demonstrate the positive relationship
421 between the profiles of increased genetic requirements for hypoxic metabolic
422 remodeling and the phenotypes advantageous for bacterial survival under hypoxic
423 conditions.

424 In this study, 121 genes were detected as significantly reduced Tn insertion in the
425 clinical MAC-PD strains compared to ATCC13950, which was higher than the case of
426 Mtb showing 10–50 genes with altered Tn insertion reads detected by a resampling
427 analysis[8]. This may reflect the genomic diversity of *M. intracellulare* compared with
428 that of Mtb. The proportion of accessory genes is larger in NTM than in Mtb[33]. In a
429 clinical trial of phage therapy for *M. abscessus* infection, the number of accessory genes
430 was shown to decrease with the loss of virulence in *M. abscessus* during the course of
431 therapy[34], suggesting some role for accessory genes for its clinical pathogenesis. Our
432 data of the overlap of the accessory essential or growth-defect-associated genes such as

433 *pckA* and *mycP5* (Supplementary Table 7) with genes required for mouse lung infection
434 (Fig. 6b, Supplementary Fig. 3) supports the idea that accessory genes (non-core genes)
435 may encode functions required for bacterial survival, especially under nonoptimal
436 conditions, such as hypoxia and during the infection of human and animal bodies.
437 Our TnSeq data are consistent with metabolomic data that have shown the
438 importance of the gluconeogenic carbon flow of TCA cycle intermediates for bacterial
439 growth under hypoxic conditions in terms of the essentiality of PckA and the reverse
440 TCA cycle[35–38]. Gluconeogenesis is essential for bacterial growth when fatty acids are
441 used as a major nutrient[37]. PckA catalyzes the conversion of the metabolites derived
442 from the TCA cycle to the metabolites of gluconeogenesis[36]. The reaction catalyzed by
443 PckA is essential for bacterial growth when the available nutrients are predominantly
444 fatty acids[39,40]. The main nutrients for mycobacteria inside hypoxic granulomas in an
445 infected human or mouse body are lipids, such as fatty acids and cholesterol, rather than
446 carbohydrates[37,41]. In the present study, *M. intracellulare* grew under 5% oxygen,
447 whereas Mtb stops growing under 1% oxygen and enters a dormant state[36]. The
448 depletion of phosphoenolpyruvate in the *pckA* deletion mutant of Mtb reduced the
449 phosphoenolpyruvate–carbon flux essential for bacterial growth and drug sensitivity[36].
450 The present study supports the idea that PckA is essential for the microaerobic growth

451 of mycobacteria. Our TnSeq data imply the preferential adaptation of the clinical MAC-
452 PD strains for circumstances *in vivo*, which are characterized by hypoxia.
453 On the other hand, such metabolic shift towards gluconeogenesis and reverse TCA
454 cycle can also be observed under reactive nitrogen species and *in vivo* infection as well.
455 This suggests that the metabolic shift observed under hypoxia is a general stress
456 response rather than being specific to hypoxia due to the nature of the
457 provided/available carbon source[42]. Several factors other than hypoxia can be estimated
458 to be related to the change of the genetic requirements in the clinical MAC-PD strains
459 such as host-related factors and general stress conditions (i.e. nutrition of abundant fatty
460 acids and less carbohydrates, low pH circumstances)[37,39-41]. Except for our data of the
461 profile of genes required for hypoxic pellicle formation in *M. intracellulare*[10], no
462 fundamental genome-wide data are available on the change of the genetic requirements
463 in response to each stress factor in non-tuberculous mycobacteria. Further studies are
464 needed to discriminate which factors are specifically involved in the increased
465 requirements of each gene. Although of interest, it is beyond the scope of the current
466 study.
467 As in the *glpX*-knockdown strains, *csd* knockdown caused growth suppression in
468 several MAC-PD strains. This type II Csd is involved in the biosynthesis of the iron–

469 sulfur clusters of the SUF machinery. Compared with the type I cysteine desulfurase
470 IscS, the SUF machinery is active under oxidative-stress and iron-limiting conditions[50].
471 Representatives of iron–sulfur cluster proteins include components of the electron-
472 transport system, such as NADH dehydrogenase I (Nuo) and succinate dehydrogenase
473 (Sdh), which are components of respiratory complexes I and II, respectively. Under
474 hypoxic conditions, the non-proton-translocating type II NADH dehydrogenase Ndh is
475 upregulated, and cytochrome *bd* oxidase (CydAB) and the proton-pumping type I
476 NADH dehydrogenase (Nuo) are downregulated[42]. In the reverse TCA cycle on the
477 same reaction pathway as Sdh, fumarate reductase (Fnr) is also an iron–sulfur cluster
478 protein that produces succinate, and is a proposed alternative electron acceptor under
479 hypoxic conditions[38,51]. The increased essentiality of the *csd* gene observed in the
480 clinical MAC-PD strains seems to reflect the switching of the electron-transport system
481 to less-energy-efficient respiration to support preferential hypoxic survival, including *in*
482 *vivo*.

483 About 10% of the genes required for mouse infection are also required for hypoxic
484 pellicle formation. The genes showing increased genetic requirements in the clinical
485 MAC-PD strains, such as *pckA* and genes encoding the ESX-5 type VII secretion
486 system, including *eccC5* and *mycP5*, also showed increased genetic requirements in

487 mouse infections. In a TnSeq study of mice infected intravenously with *M. avium*, the
488 genes of the ESX-5 type VII secretion system were required for infection of the liver
489 and spleen[43]. The ESX-5 type VII secretion system is involved in the transport of fatty
490 acids and the virulence of mycobacteria[44,45]. These similarities in the profiles of genetic
491 requirements prompt us to propose some role of biofilm formation in mycobacterial
492 pathogenesis in animals and humans. In the present study, we shed light on the impact
493 of hypoxia on biofilm formation, the acquisition of virulence, and the *in vivo*
494 pathogenesis of NTM in terms of global genetic requirements. Although the
495 morphologies of the pellicle and macroscopic lesions (including cavitation and nodular
496 bronchiectasis) are not similar, monitoring the expression of the genes identified in this
497 study may provide clues to the mechanism of biofilm formation *in vivo*.
498 The data of validation of the universal essential or growth-defect associated genes
499 by the CRISPR-i system was overall acceptable in the clinically MAC-PD strains whose
500 knockdown strains could be constructed (Fig. 7a). However, we have encountered the
501 difficulties of validating the TnSeq-hit genes by CRISPR-i experiment, especially
502 accessory and strain-dependent essential or growth-defect-associated genes in the
503 MAC-PD strains other than M.i.198 or M003 (Fig. 7b, Supplementary Fig. 7). We found
504 the lower efficiency of the suppression of gene expression by CRISPR-i in *M.*

505 *intracellulre* than in Mtb that is reported to be suppressed to 6% under 10 ng/ml

506 anhydrotetracycline (aTc) and by < 1% under 100 ng/ml aTc in the knockdown strains,

507 compared to strains expressing scrambled single guide RNAs (sgRNA)[32]. However,

508 because the levels of knockdown efficiency were comparable between strain-

509 dependent/accessory essential genes and universally essential genes (Supplementary

510 Fig. 8), the low efficiency of knockdown does not seem to explain the reason of the

511 discrepancy between TnSeq and CRISPR-i results. Although it is difficult to find the

512 clear definitive reason for this phenomenon only from the current study, the possible

513 reason may be speculated by the bypass mechanism of gene essentiality which is

514 characteristically observed in strain-dependent/accessory essential or growth-defect-

515 associated genes. According to the publication by Rosconi[14] reporting the 'forced-

516 evolution experiments' of 36 clinical *Streptococcus pneumoniae* strains., gene

517 essentiality can be bypassed by several mechanisms including the composition of the

518 accessory genome and pathway rewiring, They recovered successfully knockout

519 mutants from transformation experiments in strain-dependent/accessory essential genes

520 such as cytidine monophosphate kinase, a folate pathway enzyme formate

521 tetrahydrofolate ligase and an undecaprenyl phosphate-biosynthesis pathway enzyme

522 farnesyl-diphosphate synthase. The bypassing of gene essentiality could be suggested

523 by observing suppressor mutations and synthetic lethality in knockout strains. By
524 contrast, universal essential genes were reported to fulfill the three categories including
525 high levels of conservation within and often across species, limited genetic diversity,
526 and high and stable expression levels. Consequently, universal essential genes were
527 estimated to be rigid, largely immutable key components to an organism's survival. The
528 knockout recovery of the universal essential genes was reported to fail as shown by no
529 colonies or only appearance of merodiploids. Taking into consideration such bypass
530 mechanism of gene essentiality, the inconsistent effect of gene silencing of strain-
531 dependent/accessory essential genes on bacterial growth may reflect some kinds of
532 pathway rewiring that helps the bacteria grow under suppression of the target gene
533 expression. Nevertheless, our study has opened the avenue for functional analysis of
534 NTM that leads to the development of novel drugs targeting universal and
535 accessory/strain-dependent essential metabolic pathways, especially by making use of
536 M.i.198 and M003 as optimal NTM strains for gene manipulation.

537 In this study, we revealed the pattern of hypoxic adaptation characteristic to the
538 clinical MAC-PD strains by the growth curve analysis: an early entry to log phase
539 followed by a reduced growth rate (Fig. 8). This pattern implicates the continuous impact
540 on the infected hosts during logarithmic bacterial growth, which may be involved in the

541 persistent and steadily progressive illness for years in humans[3]. The advantage of slow
542 growth in mycobacteria may be inferred by the role of a histone-like nucleoid protein,
543 mycobacterial DNA-binding protein 1 (MDP1), also designated HupB[46-48]. The
544 expression of MDP1 is enhanced in the stationary phase, resulting in reduced growth
545 speed and long-term survival with increased resistance to reactive oxygen species
546 (ROS)[46-48]. The reduced growth rate after entry to log phase may allow long-term survival
547 of mycobacteria under ROS-rich circumstances inside host cells. The pattern of hypoxic
548 adaptation as observed in the clinical MAC-PD strains may enhance pathogenesis by
549 extending the period of the repeated process of bacterial invasion and replication in
550 infected macrophages.

551 Contrary to our expectation, not all clinical strains showed rapid adaptation from
552 aerobic to hypoxic conditions relative to ATCC13950. The two strains belonging to the
553 MP-MIP subgroup, MOTT64 and M001 showed similar time at midpoint under aerobic
554 conditions. However, the time at midpoint was significantly different between MOTT64
555 and M001 under hypoxia, the latter showing great delay of timing of entry to
556 logarithmic phase. In contrast to the majority of the clinical strains that showed slow
557 growth at midpoint under hypoxia, neither strain showed such phenomenon. These data
558 suggest that some, but not a major proportion of, clinical *M. intracellulare* strains do not

559 have an advantageous phenotype for continuous logarithmic growth under hypoxia. In
560 Mtb, the adaptation to hypoxia is considered to be necessary for clinical pathogenesis
561 because the conditions *in vivo*, such as inside macrophages or granulomas, are
562 hypoxic[42,49]. Our inability to construct knockdown strains in M001 and MOTT64
563 prevented us from clarifying the factors that discriminate against the pattern of hypoxic
564 adaptation. Although the implication in clinical situations has not been proven, strains
565 without slow growth under hypoxia may have different (possibly strain-specific)
566 mechanisms of hypoxic adaptation corresponding to their growth phenotypes under
567 hypoxia. Nevertheless, because we have shown that most of the *M. intracellulare* strains
568 with different genotypes showed preferential adaptation to hypoxia in this study, our
569 results largely reflect the clinical situation of the etiological agents of MAC-PD. A
570 possible strategy for identifying factors that confer clinical pathogenesis will be to focus
571 on the major clinical strains that show preferential hypoxic adaptation.
572 We tried to use inhibitors of phosphoenolpyruvate carboxykinase to confirm the
573 increased essentiality of the *pckA* gene. However, we detected no positive effect because
574 millimolar 3-mercaptopicolinic acid is required to show the effect of inhibition, even in
575 eukaryotic cells, which have no cell wall[52]. Moreover, 3-alkyl-1,8-dibenzylxanthine[53]
576 also only effectively inhibits PckA in eukaryotic cells. However, PckA has been

577 proposed as a drug target for Mtb[54], so our TnSeq data seem to be consistent with
578 studies directed towards antimycobacterial drug discovery.

579 We found the difference in capacity of transformation between strains belonging to
580 the same genomic *M. paraintracellulare-M. indicus pranii* (MP-MIP) subgroup.
581 Although the direct mechanism determining the competency for foreign DNA has not
582 been elucidated in *M. intracellulare* and other NTM species, several studies on general
583 bacteria suggest the difficulties of introducing foreign DNA into clinical strains
584 compared to the laboratory strains. As suggested in *Staphylococcus aureus*[55], some
585 clinical strains develop elimination systems of foreign nucleic acids such as a type III-
586 like restriction endonuclease. As suggested in gran-negative bacteria[56], there may be
587 some difference in cell surface structures between strains, resulting in the necessity of
588 polymyxin B nonapeptide targeting cell membrane for transforming clinical strains. The
589 efficiency of eliminating foreign DNA may be attributed to various kinds of strain-
590 specific factors including restriction endonuclease, natural CRISPR-interference system
591 and cell wall structures rather than a simple genotype factor.

592 There may be a claim that the saturation of Tn insertion in most of each replicate
593 were 50-60% in our libraries. However, our method of constructing Tn mutant libraries
594 is in accordance with the previous studies of "high-density" transposon libraries[9]

595 because the saturation of the Tn mutant libraries by combining replicates are 62-79% as
596 follows: ATCC13950: 67.6%, M001: 72.9%, M003: 63.0%, M018: 62.4%, M019:
597 74.5%, M.i.27: 76.6%, M.i.198: 68.0%, MOTT64: 77.6%, M021: 79.9%. That is, we
598 predicted gene essentiality from the Tn mutant libraries with 62-79% saturation in each
599 strain. However, there is non-permissive sequence pattern in mariner transposon
600 mutagenesis and using more than 10 replicates of Tn mutant libraries is reported to be a
601 more accurate method[57,58]. The issue of high probability of judging nonessential region
602 as mistakenly as "essential" are mainly found in small ORFs (2-9 TA sits) rather than
603 larger ORFs (TA sites > = 10))[57]. There are 4136 (6.43% of total ORFs) nonpermissive
604 TA sites in ATCC13950, which is less than in *M. tuberculosis* H37Rv (9% of total
605 ORFs)[57] and in *M. abscessus* ATCC19977 (8.1% of total ORFs)[58]. As for small ORFs
606 (2-9 TA sites), there are nonpermissive TA sites in 41 genes (ORFs) of common
607 essential or growth-defect- associated (1.35% of a total of 3021 larger ORFs in
608 ATCC13950). With respect to the covering of non-permissive sites, our TnSeq data may
609 need to be improved to classify quite accurately the gene essentiality particularly on the
610 nonstructural small regulatory genes including small RNAs, although the study by
611 DeJesus shows the comparable number of essential genes in large genes possessing
612 more than 10 TA sites between 2 and 14 TnSeq datasets, most of which seem to be

613 structural genes[57].

614 We have provided the data suggesting the preferential hypoxic adaptation in clinical
615 strains compared to the ATCC type strain by the growth assay of individual strains. To
616 strengthen our claim, several experiments are suggested including mixed culture
617 experiments of clinical and reference strains under hypoxia. However, co-culture
618 conditions introduce additional variables, including inter-strain competition or synergy,
619 which can obscure the specific contributions of hypoxic adaptation in each strain.
620 Therefore, we took the current approach using monoculture growth curves under
621 defined oxygen conditions, which offers a clearer interpretation of strain-specific
622 hypoxic responses. Furthermore, one of the limitations of this study is the lack of
623 validation of TnSeq results with individual gene knockouts. Contrary to the case of Mtb,
624 the technique of constructing knockout mutants of slow-growing NTM including *M.*
625 *intracellulare* has not been established long time. We have just recently succeeded in
626 constructing the vector plasmids for making knockout mutants of *M intracellulare*[59].
627 Growth assay of individual knockout strains of genes showing increased genetic
628 requirements such as *pckA*, *glpX*, *csd*, *eccC5* and *mycP5* in the clinical strains is
629 suggested to provide the direct involvement of these genes on the preferential hypoxic
630 adaptation in clinical strains. We have a future plan to construct knockout mutants of

631 these genes to confirm the involvement of these genes on preferential hypoxic
632 adaptation.
633 In summary, we have identified 131 universal essential and growth-defect-
634 associated genes that cover the genomic diversity of *M. intracellulare* strains
635 responsible for MAC-PD, which narrowed down the drug targets against MAC-PD.
636 Furthermore, we have demonstrated preferential adaptation to hypoxia in clinical NTM
637 strains compared with the type strain in terms of the increased genetic requirements for
638 hypoxic growth, such as those encoding phosphoenolpyruvate carboxykinase, the ESX-
639 5 type VII secretion system, and cysteine desulfurase. These genes were shown to have
640 a significant impact on infection *in vivo* by increasing their genetic requirements. Our
641 data highlight the importance of using clinical strains and hypoxic conditions in
642 experimental research, and provide fundamental resources for developing novel drugs
643 directed towards nontuberculous mycobacterial strains that cause severe clinical
644 diseases.
645

646 **Methods**

647 **Bacterial strains and phages used to prepare Tn mutants**

648 A total of eleven strains were used in this study, including nine clinical strains isolated

649 from patients with MAC-PD in Japan (M.i.198, M.i.27, M018, M003, M019, M021,

650 M001, M005, M016)[22], *M. intracellulare* genovar *paraintracellulare* type strain

651 MOTT64 isolated from MAC-PD in South Korea[60]and the *M. intracellulare* type strain

652 ATCC13950 (Fig. 1, Supplementary Table 1). All eleven clinical strains from MAC-PD

653 patients in Japan were isolated from sputum[5,22]. Sputum samples were treated by the

654 standard method for clinical isolation of mycobacteria with 0.5% (w/v) N-acetyl-L-

655 cysteine and 2% (w/v) sodium hydroxide and plated on 7H10/OADC agar. Single

656 colonies were picked up for use in experiments as isolated strains. Of these strains,

657 ATCC13950, M.i.198, M.i.27, M018, M005 and M016 belong to the typical *M.*

658 *intracellulare* (TMI) genotype and M001, M003, M019, M021 and MOTT64 belong to

659 the *M. paraintracellulare-M. indicus pranii* (MP-MIP) genotype (Fig. 1, Supplementary

660 Table 1). The Tn mutant libraries were constructed using glucose as a carbon source

661 under aerobic conditions according to the transduction method used for ATCC13950[10],

662 except that a higher concentration of kanamycin (100 μg/ml) was used to select the

663 transposon mutants than was used for ATCC13950 (25 μg/ml). In brief, a hundred

664 milliliter of the bacteria were cultured aerobically in Middlebrook 7H9 medium (Difco

665 Laboratories, Detroit, MI, USA) containing 0.2% glycerol, 0.1% Tween 80 (MP

666 Biochemicals, Illkrich, France), and 10% Middlebrook albumin–dextrose–catalase

667 (7H9/ADC/Tween 80) until mid-log phase (optical density at a wavelength of 600 nm

668 [OD_{600}] of approximately 0.4–0.6). After harvesting the bacteria, 10 mL of high-titer

669 mycobacteriophage phAE180[61] was transduced into the bacteria 1-day at 37°C for

670 inserting Tn and plated on Middlebrook 7H10 solid medium supplemented with 10%

671 oleic acid-albumin-dextrose-catalase (Becton Dickinson and Co., Sparks, MD)

672 (7H10/OADC) agar plates containing kanamycin. After 2 or 3 week-cultivation at 37°C

673 aerobically, the colonies were harvested *en masse* and used as Tn mutant libraries. The

674 kanamycin-resistant colonies (> 1×10^5) were harvested and evenly resuspended in

675 7H9/ADC medium containing 20% glycerol, aliquoted, and stored at −80 °C until

676 further use.

677 **Next-generation sequencing and TnSeq analysis**

678 DNA libraries were prepared as reported previously[62]. The TnSeq libraries were

679 sequenced with the NextSeq 500 System, 150-bp single-end run (Illumina, San Diego,

680 CA, USA). The sequence reads were analyzed as previously described[10]. Genetic

681 requirements were calculated, and gene essentiality was predicted by resampling and

682 HMM analyses using TRANSIT, respectively[12]. First, an HMM analysis was conducted

683 to calculate the fluctuation of the number of Tn insertion reads individually for each

684 strain. HMM method can categorize the gene essentiality throughout the genome

685 including “Essential”, “Growth-defect”, “Non-essential” and “Growth-advantage”.
686 “Essential” genes are defined as no insertions in all or most of their TA sites. “Non-
687 essential” genes are defined as regions that have usual read counts. “Growth-defect”
688 genes are defined as regions that have unusually low read counts. “Growth-advantage”
689 genes are defined as regions that have unusually high low read counts. Universal
690 essential and growth-defect-associated genes were identified as the genes classified as
691 “Essential” and “Growth-defect” with an HMM analysis in all 9 subject strains
692 (Supplementary Table 4). Next, a resampling analysis was conducted to calculate the
693 difference of the number of Tn insertion reads between each clinical strain and
694 ATCC13950 (Supplementary Table 8). By comparing the data obtained by HMM and
695 resampling analyses, we summarized the difference of genetic requirements between the
696 clinical MAC-PD strains and ATCC13950. To compare the genetic requirements of the
697 clinical MAC-PD strains and ATCC13950, the annotation for the clinical MAC-PD
698 strains was adapted from that of ATCC13950 by adjusting the START and END
699 coordinates of each open reading frame (ORF) in the clinical MAC-PD strains
700 according to their alignment with the corresponding ORFs of ATCC13950. The number
701 of Tn insertion in our datasets varied between 1.3 to 5.8 million among strains. To
702 reduce the variation in the Tn insertion across strains, we adopt a non-linear

703 normalization method, Beta-Geometric correction (BGC). BGC normalizes the datasets
704 to fit an "ideal" geometric distribution with a variable probability parameter ρ[12], and
705 BGC improves resampling by reducing the skew. On TRANSIT software, we set the
706 replicate option as Sum to combine read counts. And we normalized the datasets by
707 BGC and performed resampling analysis by using normalized datasets to compare the
708 genetic requirements between strains. The function of TnSeq-hit genes was categorized
709 according to the Kyoto Encyclopedia of Genes and Genomes (KEGG) database.

710 **Animals**

711 Female C57BL/6JJcl mice were purchased from CLEA Japan (Tokyo, Japan). Six-
712 week-old mice were used for the infection experiment (Supplementary Fig. 3). All the
713 mice were kept under specific-pathogen-free conditions in the animal facility of Niigata
714 University Graduate School of Medicine, according to the institutional guidelines for
715 animal experiments. The mice were housed (four per cage) under a 12-h/12-h light/dark
716 cycle. Food and water were available *ad libitum*. Kanamycin was added to the drinking
717 water to a final concentration of 100 μg/ml to maintain the mice's resistance to the Tn
718 mutant strains. Euthanasia was conducted with an intraperitoneal injection of a
719 combined anesthetic (15 μg of medetomidine, 80 μg of midazolam, and 100 μg of
720 butorphanol), followed by cervical dislocation.

721 **Mouse TnSeq experiment**

722 The protocol was based on our previous mouse lung infection experiment[22]. Twenty
723 mice each were used for the Tn mutant strains M.i.198 and M.i.27. The mice were
724 injected intratracheally with 3.25×10^8 and 5.93×10^7 CFUs of the Tn mutant strains,
725 respectively. The infected lungs were expected to be harvested from five mice at day 1,
726 week 4, week 8, and week 16 after infection. However, the lungs were harvested from
727 only four mice infected with the M.i.27 Tn mutant strains in week 8 because we
728 experienced difficulties with sampling, and the lungs were harvested from only three,
729 one, and two mice infected with M.i.198 Tn mutant strains in week 8, week 12, and
730 week 16, respectively, because morbidity was high in the mice infected with M.i.198.
731 The harvested lungs were homogenized in 4.5 ml of distilled water with the
732 gentleMACS™ Tissue Dissociator (Miltenyi Biotec, Bergish Gladbach, Germany) and
733 the homogenates were plated on 7H10/OADC agar plates and cultured for 3 weeks. The
734 colonies were harvested *en masse* for TnSeq.

735 **Gene set enrichment analysis**

736 To investigate the overlap of the gene sets required for growth in mouse lungs with
737 those required for hypoxic pellicle formation observed in ATCC13950 and those
738 showing increased genetic requirements observed in the clinical MAC-PD strains, a

739 statistical enrichment of gene sets was performed by GSEA 4.3.2[15]. Parameters set for
740 GSEA were as follows: permutations = 1,000, permutation type: gene_set, enrichment
741 statistic: weighted, metric for ranking genes: Signal2Noise, max size: 500, min size: 15.

742 **Construction and growth assay of knockdown strains**

743 Knockdown strains were constructed with the CRISPR-dCas9-mediated RNA
744 interference system, as reported previously[29]. Gene-specific 20-nt sequences were
745 selected as protospacers for incorporation into the sgRNAs (Supplementary Table 20).
746 pRH2502 (a vector expressing an inactivated version of the *cas9* DNA sequence) and
747 pRH2521 (an sgRNA-expressing vector whose expression is regulated by the TetR-
748 regulated smyc promotor P_{myc1}tetO) were introduced into the bacteria to obtain colonies
749 of the knockdown strains. For selection, 25 μg/ml kanamycin and 50 μg/ml hygromycin
750 were used for ATCC13950, and 100 μg/ml kanamycin and 50 μg/ml hygromycin were
751 used for the clinical strains. The growth assay of the knockdown strains was performed
752 in 7H9/ADC broth containing the above-mentioned concentrations of kanamycin and
753 hygromycin under aerobic conditions at 37 °C with humidification (APM-30D
754 incubator, Astec, Tokyo, Japan). During the assay, the cultures were supplemented with
755 anhydrotetracycline (aTc) to a final concentration of 50 ng/ml (as a concentration that is
756 not toxic to ATCC13950 and M.i.27) or 200 ng/ml (for the other clinical strains). aTc

757 was added repeatedly every 48 h to maintain the induction of dCas9 and sgRNAs in
758 experiments that extended beyond 48 h[29]. An aliquot (4 µl) of the culture and its diluents
759 were streaked onto 7H10/OADC agar plates containing kanamycin and hygromycin,
760 and the CFUs were counted. Growth inhibition was evaluated as the ratio of the CFUs
761 of knockdown strains compared with those of the vector control strains lacking the
762 guide RNA sequence. To confirm the downregulation of gene expression in the
763 knockdown strains, quantitative reverse transcription PCR (qRT-PCR) was performed.
764 Bacteria were cultured in 10 ml of 7H9/ADC/Tween 80 containing kanamycin and
765 hygromycin until mid-log phase (OD_{600} approximately 0.4–0.6). The cultures were
766 supplemented with aTc every 48 h, as in the growth assay for the knockdown strains.
767 One day after the second addition of aTc, RNA was extracted by bead-beating six times
768 at 5000 rpm for 30 s with cooling (Micro Smash MS 100R Cell Disruptor; Tomy Seiko,
769 Tokyo, Japan) and cDNA was synthesized with the Direct-zol™ RNA Miniprep (Zymo
770 Research, Orange, CA, USA) and ReverTra Ace qPCR RT Master Mix with gDNA
771 Remover (Toyobo, Osaka, Japan). qRT-PCR was performed with the CFX Connect
772 Real-time PCR Detection System (Bio-Rad, Hercules, CA, USA), according to the
773 manufacturer's instructions. The data were normalized to the expression of *sigA*.
774 **Comparison of growth curves under aerobic and hypoxic conditions**

775 First, we precultured the bacteria in 7H9/ADC broth until the bacteria reached early log-
776 phase (OD_{600} approximately 0.1–0.3). Next, the bacterial cultures were diluted with new
777 7H9/ADC broth (final OD_{600} 0.003) for the aerobic and hypoxic growth assay. Bacterial
778 cells were grown statically in 96-well plates containing 250 μl of 7H9/ADC broth in
779 each well under aerobic conditions or 5% oxygen at 37 °C with humidification (APM-
780 30D incubator, Astec, Tokyo, Japan). The culture was sampled every 1–3 days. At
781 sampling, the culture was mixed by pipetting 50 times. An aliquot (4 μl) of the culture
782 and its diluents were streaked onto 7H10/OADC agar and the CFUs counted. The
783 growth curve was fitted to the logistic 4P model with the JMP software (SAS Institute
784 Inc., Cary, NC, USA) to calculate the inflection point (midpoint) and growth rate at
785 midpoint in the log growth phase. Entry into the log phase was evaluated from the
786 timing of the inflection point on the growth curve.

787 **Statistical analyses**

788 The cut-off of fold-change (log_2FC) to compare genetic requirements by TnSeq
789 resampling analysis was set as adjusted *P*-values less than 0.05. Pearson's correlation
790 test was performed between the fitness costs (log_2FC calculated by the resampling
791 assay), efficiency of knockdown (assessed by qRT-PCR) and growth suppression in the
792 knockdown strains. Statistical analyses of the growth curves were performed using a 4-

793 parameter logistic model (logistic 4P model), Wilcoxon two-sample test, and a one-way

794 analysis of variance (ANOVA) followed by Steel's multiple comparisons test using the

795 JMP software program (SAS Institute Inc., Cary, NC, USA). Data are presented as the

796 mean ± SD. Statistical significance was set as *P* values less than 0.05.

797

[References]

1. Adjemian, J., Olivier, K.N., Seitz, A.E., Holland, S.M. & Prevots, D.R. Prevalence of nontuberculous mycobacterial lung disease in U.S. Medicare beneficiaries. *Am J Respir Crit Care Med* **185**, 881-886 (2012).

2. Namkoong, H. *et al.* Epidemiology of pulmonary nontuberculous mycobacterial disease, Japan. *Emerg Infect Dis* **22**, 1116-1117 (2016).

3. Daley, C.L. *et al.* Treatment of nontuberculous mycobacterial pulmonary disease: an official ATS/ERS/ESCMID/IDSA clinical practice guideline. *Eur Respir J* **56**, 2000535 (2020).

4. Uchiya, K.I. *et al.* Comparative genome analyses of *Mycobacterium avium* reveal genomic features of its subspecies and strains that cause progression of pulmonary disease. *Sci Rep* **7**, 39750 (2017).

5. Tateishi, Y. *et al.* Comparative genomic analysis of *Mycobacterium intracellulare*: implications for clinical taxonomic classification in pulmonary *Mycobacterium avium-intracellulare* complex disease. *BMC Microbiol* **21**, 103 (2021).

6. Tortoli, E. *et al.* Genome-based taxonomic revision detects a number of synonymous taxa in the genus *Mycobacterium*. *Infect Genet Evol* **75**, 103983 (2019).

817 7. van Opijnen, T. & Camilli, A. Transposon insertion sequencing: a new tool for
818 systems-level analysis of microorganisms. *Nat Rev Microbiol* **11**, 435-442
819 (2013).
820 8. Carey, A.F. *et al.* TnSeq of *Mycobacterium tuberculosis* clinical isolates reveals
821 strain-specific antibiotic liabilities. *PLoS Pathog* **14**, e1006939 (2018).
822 9. Akusobi, C. *et al.*. Transposon-sequencing across multiple *Mycobacterium*
823 *abscessus* isolates reveals significant functional genomic diversity among
824 strains. *mBio* **6**, e0337624 (2025).
825 10. Tateishi, Y. *et al.* Genome-wide identification of essential genes in
826 *Mycobacterium intracellulare* by transposon sequencing - Implication for
827 metabolic remodeling. *Sci Rep* **10**, 5449 (2020).
828 11. Cuttino, J.T. & Mc, C.A. Pure granulomatous nocardiosis, a new fungus disease
829 distinguished by intracellular parasitism; a description of a new disease in man
830 due to a hitherto undescribed organism, *Nocardia intracellularis*, n. sp.,
831 including a study of the biologic and pathogenic properties of this species. *Am J*
832 *Pathol* **25**, 1-47 (1949).
833 12. DeJesus, M.A., Ambadipudi, C., Baker, R., Sassetti, C. & Ioerger, T.R.
834 TRANSIT--A software tool for Himar1 TnSeq analysis. *PLoS Comput Biol* **11**,

835 e1004401 (2015).

836 13. Krieger, I.V. *et al.* Structure-guided discovery of phenyl-diketo acids as potent
837 inhibitors of *M. tuberculosis* malate synthase. *Chem Biol* **19**, 1556-1567 (2012).

838 14. Rosconi, F. *et al.* A bacterial pan-genome makes gene essentiality strain-
839 dependent and evolvable. *Nat Microbiol* **7**, 1580–1592 (2022).

840 15. Subramanian, A. *et al.* Gene set enrichment analysis: A knowledge-based
841 approach for interpreting genome-wide expression profiles. *Proc Natl Acad Sci*
842 *U S A* **102,** 15545–15550 (2005).

843 16. Coll, F. *et al.* Genome-wide analysis of multi- and extensively drug-resistant
844 *Mycobacterium tuberculosis*. *Nat Genet* **50**, 307-316 (2018).

845 17. Nguyen, H.T., Wolff, K.A., Cartabuke, R.H., Ogwang, S. & Nguyen, L. A
846 lipoprotein modulates activity of the MtrAB two-component system to provide
847 intrinsic multidrug resistance, cytokinetic control and cell wall homeostasis in
848 *Mycobacterium*. *Mol Microbiol* **76**, 348-364 (2010).

849 18. Li, S. *et al.* CRISPRi chemical genetics and comparative genomics identify
850 genes mediating drug potency in *Mycobacterium tuberculosis*. *Nat Microbiol* **7**,
851 766–779 (2022).

852 19. Kirschner, R.A., Jr., Parker, B.C. & Falkinham, J.O., 3rd. Epidemiology of

853 infection by nontuberculous mycobacteria. *Mycobacterium avium,*
854 *Mycobacterium intracellulare,* and *Mycobacterium scrofulaceum* in acid, brown-
855 water swamps of the southeastern United States and their association with
856 environmental variables. *Am Rev Respir Dis* **145**, 271-275 (1992).
857 20. Werner, E. *et al.* Stratified growth in *Pseudomonas aeruginosa* biofilms. *Appl*
858 *Environ Microbiol* **70**, 6188-6196 (2004).
859 21. Via, L.E. *et al.* Tuberculous granulomas are hypoxic in guinea pigs, rabbits, and
860 nonhuman primates. *Infect Immun* **76**, 2333-2340 (2008).
861 22. Tateishi, Y. *et al.* Virulence of *Mycobacterium intracellulare* clinical strains in a
862 mouse model of lung infection - role of neutrophilic inflammation in disease
863 severity. *BMC Microbiol* **23**, 94 (2023).
864 23. Kryzywinska, E., Bhatnagar, S., Sweet, L., Chatterjee, D. & Schorey, J.S.
865 *Mycobacterium avium* 104 deleted of the methyltransferase D gene by allelic
866 replacement lacks serotype-specific glycopeptidolipids and shows attenuated
867 virulence in mice. *Mol Microbiol* **56**, 1262-1273 (2005).
868 24. Irani, V.R., Lee, S.-H., Eckstein, T.M., Inamine, J.M., Belisle, J.T. & Maslow,
869 J.N. Utilization of a *ts-sacB* selection system for the generation of a
870 *Mycobacterium avium* serovar-8 specific glycopeptidolipid allelic exchange

871 mutant. A*nnals Clin Microbiol Antimicrob* **3**, 18 **(**2004).

872 25. Marklund, B.I., Speert, D.P. & Stokes, R.W. Gene replacement through

873 homologous recombination in *Mycobacterium intracellulare*. *J Bacteriol* **177**,

874 6100-6105 (1995).

875 26. Marklund, B.I., Mahenthiralingam, E. & Stokes, R.W. Site-directed mutagenesis

876 and virulence assessment of the *katG* gene of *Mycobacterium intracellulare*. *Mol*

877 *Microbiol* **29**, 999-1008 (1998).

878 27. Mahenthiralingam, E., Marklund, B.I., Brooks, L.A., Smith, D.A., Bancroft, G.J.

879 & Stokes, R.W. Site-directed mutagenesis of the 19-kilodalton lipoprotein

880 antigen reveals No essential role for the protein in the growth and virulence of

881 *Mycobacterium intracellulare*. *Infect Immun*. **66**, 3626-3634 (1998).

882 28. Hinds, J. *et al.* Enhanced gene replacement in mycobacteria. *Microbiology* **145**,

883 519-527 (1999).

884 29. Singh, A.K. *et al.* Investigating essential gene function in *Mycobacterium*

885 *tuberculosis* using an efficient CRISPR interference system. *Nucleic Acids Res*

886 **44**, e143 (2016).

887 30. Choudhary, E., Thakur, P., Pareek, M. & Agarwal, N. Gene silencing by CRISPR

888 interference in mycobacteria. *Nat Commun* **6**, 6267 (2015).

889 31. Rock, J.M. *et al.* Programmable transcriptional repression in mycobacteria using
890 an orthogonal CRISPR interference platform. *Nat Microbiol* **2,** 16274 (2017).
891 32. McNeil, M.B. & Cook, G.M. Utilization of CRISPR interference to validate
892 MmpL3 as a drug target in *Mycobacterium tuberculosis*. *Antimicrob Agents*
893 *Chemother* **63,** e00629-19 (2019).
894 33. Yang, T. *et al.* Pan-genomic study of *Mycobacterium tuberculosis* reflecting the
895 primary/secondary genes, generality/individuality, and the interconversion
896 through copy number variations. *Front Microbiol* **9**, 1886 (2018).
897 34. Nick, J.A. *et al.* Host and pathogen response to bacteriophage engineered against
898 *Mycobacterium abscessus* lung infection. *Cell* **185**, 1860-1874.e12 (2022).
899 35. Eoh, H. *et al.* Metabolic anticipation in *Mycobacterium tuberculosis*. *Nat*
900 *Microbiol* **2**, 17084 (2017).
901 36. Lim, J. *et al.* Phosphoenolpyruvate depletion mediates both growth arrest and
902 drug tolerance of *Mycobacterium tuberculosis* in hypoxia. *Proc Natl Acad Sci U*
903 *S A* **118,** e2105800118 (2021).
904 37. Marrero, J., Rhee, K.Y., Schnappinger, D., Pethe, K. & Ehrt, S. Gluconeogenic
905 carbon flow of tricarboxylic acid cycle intermediates is critical for
906 *Mycobacterium tuberculosis* to establish and maintain infection. *Proc Natl Acad*

907 *Sci U S A* **107**, 9819-9824 (2010).

908 38. Watanabe, S. *et al.* Fumarate reductase activity maintains an energized
909 membrane in anaerobic *Mycobacterium tuberculosis*. *PLoS Pathog* **7**, e1002287
910 (2011).

911 39. Gouzy, A., Healy, C., Black, K.A., Rhee, K.Y. & Ehrt, S. Growth of
912 *Mycobacterium tuberculosis* at acidic pH depends on lipid assimilation and is
913 accompanied by reduced GAPDH activity. *Proc Natl Acad Sci U S A* **118,**
914 e2024571118 (2021).

915 40. Quinonez, C.G. *et al.* The role of fatty acid metabolism in drug tolerance of
916 *Mycobacterium tuberculosis*. *mBio* **13**, e0355921 (2022).

917 41. Pandey, A.K. & Sassetti, C.M. Mycobacterial persistence requires the utilization
918 of host cholesterol. *Proc Natl Acad Sci U S A* **105**, 4376-4380 (2008).

919 42. Prosser, G. *et al.* The bacillary and macrophage response to hypoxia in
920 tuberculosis and the consequences for T cell antigen recognition. *Microbes*
921 *Infect* **19**, 177-192 (2017).

922 43. Dragset, M.S. *et al.* Global assessment of *Mycobacterium avium* subsp.
923 *hominissuis* genetic requirement for growth and virulence. *mSystems* **4,** e00402-
924 19 (2019).

925 44. Ates, L.S. *et al.* Essential role of the ESX-5 secretion system in outer membrane
926 permeability of pathogenic mycobacteria. *PLoS Genet* **11**, e1005190 (2015).
927 45. Ates, L.S. *et al.* The ESX-5 system of pathogenic mycobacteria is nvolved in
928 capsule integrity and virulence through its substrate PPE10. *PLoS Pathog* **12**,
929 e1005696 (2016).
930 46. Savitskaya, A. *et al.* C-terminal intrinsically disordered region-dependent
931 organization of the mycobacterial genome by a histonelike protein. *Sci Rep* 8, 1–
932 15 (2018).
933 47. Enany, S. *et al.* Mycobacterial DNA-binding protein 1 is critical for long term
934 survival of *Mycobacterium smegmatis* and simultaneously coordinates cellular
935 functions. *Sci Rep* 7, 1–11 (2017).
936 48. Shaban, A.K. *et al.* Mycobacterial DNA-binding protein 1 is critical for BCG
937 survival in stressful environments and simultaneously regulates gene expression.
938 *Sci Rep* 13, 14157 (2023).
939 49. Rustad, T.R., Sherrid, A.M., Minch, K.J. & Sherman, D.R. Hypoxia: a window
940 into *Mycobacterium tuberculosis* latency. *Cell Microbiol* **11**, 1151-1159 (2009).
941 50. Takahashi, Y. & Tokumoto, U. A third bacterial system for the assembly of iron-
942 sulfur clusters with homologs in archaea and plastids. *J Biol Chem* **277**, 28380-

943 28383 (2002).

944 51. Cecchini, G., Schröder, I., Gunsalus, R.P. & Maklashina, E. Succinate
945 dehydrogenase and fumarate reductase from *Escherichia coli*. *Biochim Biophys*
946 *Acta* **1553**, 140-157 (2002).

947 52. Brearley, M.C., Daniel, Z., Loughna, P.T., Parr, T. & Brameld, J.M. The
948 phosphoenolpyruvate carboxykinase (PEPCK) inhibitor, 3-mercaptopicolinic
949 acid (3-MPA), induces myogenic differentiation in C2C12 cells. *Sci Rep* **10**,
950 22177 (2020).

951 53. Montal, E.D. *et al.* Inhibition of phosphoenolpyruvate carboxykinase blocks
952 lactate utilization and impairs tumor growth in colorectal cancer. *Cancer Metab*
953 **7**, 8 (2019).

954 54. McLeod, M.J., Krismanich, A.P., Assoud, A., Dmitrienko, G.I. & Holyoak, T.
955 Characterization of 3-[(carboxymethyl)thio]picolinic acid: a novel inhibitor of
956 phosphoenolpyruvate carboxykinase. *Biochemistry* **58**, 3918-3926 (2019).

957 55. Corvaglia, A.R., François, P., Hernandez, D., Perron, K., Linder, P. & Schrenzel,
958 J. A type III-like restriction endonuclease functions as a major barrier to
959 horizontal gene transfer in clinical *Staphylococcus aureus* strains. *Proc Natl*
960 *Acad Sci U S A* **107,** 11954-11958 (2010).

961 56. Qin, J., Hong, Y., Pullela, K., Morona, R., Henderson, I.R. & Totsika, M. A
962 method for increasing electroporation competence of Gram-negative clinical
963 isolates by polymyxin B nonapeptide. *Sci Rep* **12,**:11629 (2022).
964 57. DeJesus, M.A. *et al.* Comprehensive essentiality analysis of the *Mycobacterium*
965 *tuberculosis* genome via saturating transposon mutagenesis. *mBio* **8,** e02133-16
966 (2017).
967 58. Rifat, D., Chen L., Kreiswirth, B.N. & Nuermberger, E.L. Genome-wide
968 essentiality analysis of *Mycobacterium abscessus* by aaturated rransposon
969 mutagenesis and deep sequencing. *mBio* **12,** e0104921 (2021).
970 59 Tateishi, Y., Nishiyama, A., Ozeki, Y. & Matsumoto, S. Construction of
971 knockout mutants in *Mycobacterium intracellulare* ATCC13950 strain using a
972 thermosensitive plasmid containing negative selection marker *rpsL*$^{+}$. *Microbiol*
973 *Immunol* **68,** 339-347 (2024).
974 60. Kim, B.J. *et al.* Complete genome sequence of *Mycobacterium intracellulare*
975 clinical strain MOTT-64, belonging to the INT1 genotype. *J Bacteriol* **194**, 3268
976 (2012).
977 61. Kriakov, J., Lee, S. & Jacobs, W.R., Jr. Identification of a regulated alkaline
978 phosphatase, a cell surface-associated lipoprotein, in *Mycobacterium smegmatis*.

979 *J Bacteriol* **185**, 4983-4991 (2003).

980 62. Minato, Y. *et al.* Genomewide assessment of *Mycobacterium tuberculosis*

981 conditionally essential metabolic pathways. *mSystems* **4,** e00070-19 (2019).

982 63. Shannon, P. *et al.* Cytoscape: a software environment for integrated models of

983 biomolecular interaction networks. *Genome Res* **13**, 2498-2504 (2003).

984

985 **Acknowledgments**

986 The authors thank Dr. Torin Weisbrod and Dr. William R. Jacobs, Jr. (Albert Einstein

987 College of Medicine, Bronx, NY, USA) for kindly providing mycobacterial phage

988 phAE180, and Dr. Norikazu Hara and Dr. Takeshi Ikeuchi (Department of Molecular

989 Genetics, Bioresource Science, Brain Center for Bioresources, Brain Research Institute,

990 Niigata University) for next-generation sequencing with the NextSeq 500 System. The

991 authors thank Mr. Naomi Yoshihara and Ms. Chisa Kumagai for constructing Tn mutant

992 library strains and hypoxic growth experiments, respectively. This work was supported

993 by Grants-in-Aid for Scientific Research (grant numbers 20KK0216, 21K19637, and

994 22H03115 to Yoshitaka Tateishi) from the Ministry of Health, Labour, and Welfare, of

995 Japan This work was also supported by grants from the Japanese Ministry of Education,

996 Culture, Sports, Science, and Technology, the Ministry of Health, and the Research

997 Program on Emerging Infectious Disease from the Japan Agency for Medical Research
998 and Development (23fk0108673h0501, AMED-CREST 25gm1610009h0004, and
999 JP223fa627005).

1000

1001 **Author contributions**

1002 Y.T. conceived, designed and performed the experiments. Y.O., A.N., and S.M.
1003 contributed reagents or materials. Y. Morishige., Y. Minato, and A.D.B. contributed
1004 analytical tools. Y. Morishige., Y. Minato, A.D.B., and S.M. provided critical suggestions
1005 throughout the preparation of the manuscript. Y.T. wrote the manuscript. All authors read
1006 and approved the final manuscript.

1007

1008 **Availability of data and materials**

1009 The datasets used or analyzed in this study are available from the corresponding author
1010 upon reasonable request.

1011

1012 **Declarations**

1013 **Ethics approval and consent to participate**

1014 All experimental protocols were approved by the Institutional Review Board of Niigata

University (approval numbers: 2019-0020 for the use of human tissue samples and SA00506 for experiments on live vertebrates). All experiments on humans and human samples were conducted in accordance with relevant guidelines and regulations. Informed consent was obtained from all patients. All experiments on animals were conducted in accordance with the relevant guidelines and regulations, and the study complied with the ARRIVE guidelines.

Consent for publication

According to the protocols approved by the Institutional Review Board of Niigata University mentioned above, consent for publication was obtained from the patients enrolled in this study.

Competing interests

The authors declare that they have no competing interests.

1028 **Fig. 1 Phylogenetic tree of the *M. intracellulare* strains and strategy of the TnSeq**
1029 **analyses in this study. a** Phylogenetic tree of the *M. intracellulare* strains used in this
1030 study. The tree was generated based on average nucleotide identity (ANI) with the
1031 neighbor-joining method. TMI: typical *M. intracellulare*; MP-MIP: *M.*
1032 *paraintracellulare–M. indicus pranii*. The detail of phylogenetic tree is shown in
1033 Supplementary Fig. 1. **b** Strategy of the procedure of TnSeq analyses.
1034
1035 **Fig. 2 Identification of the essential and growth-defect-associated genes across**
1036 genetically diverse nine ***M. intracellulare* strains used in this study. a** Functional
1037 categories of 131 genes identified as universal essential or growth-defect-associated with
1038 an HMM analysis. The genes were categorized according to the Kyoto Encyclopedia of
1039 Genes and Genomes (KEGG) database. **b** Universal essential or growth-defect-associated
1040 genes corresponding to the genes of existing antituberculous drug targets. **c** The number
1041 of the essential or growth-defect-associated genes in the accessory genes, and the number
1042 of strain-dependent essential or growth-defect-associated genes in the core genes.
1043
1044 **Fig. 3 Detection of genes showing increased or reduced genetic requirements in the**
1045 **clinical *M. intracellulare* strains.** Left panel shows the genes identified as having fewer

1046 Tn insertion reads than the type strain ATCC13950. The fold changes in the number of
1047 Tn insertion reads calculated by a resampling analysis are represented by the color scale.
1048 Red squares indicate genes required for hypoxic pellicle formation in ATCC13950[10].
1049 *Genes identified with a combination of resampling and HMM analyses. †Genes
1050 identified only with resampling analysis. Right panel shows the genes identified as having
1051 more Tn insertion reads than the type strain ATCC13950. NH: no homolog with
1052 ATCC13950, NS: no significant increase in Tn insertion reads by a resampling analysis
1053 (adjusted $P < 0.05$).
1054
1055 **Fig. 4 Overview of the differences in genetic requirements between the clinical *M.***
1056 ***intracellulare* strains and ATCC13950, drawn with Cytoscape[63].** Each central node
1057 represents the functional category of genes, assigned with a KEGG pathway analysis.
1058 Each peripheral node represents the genes showing significant changes in the number of
1059 Tn insertion reads. The size of each node represents the number of strains identified. Each
1060 edge represents a strain identified as showing significant changes in the number of Tn
1061 insertion reads. The thickness of each edge represents the adjusted *P* value. The color
1062 scale of each edge represents the fold change in the number of Tn insertion reads
1063 calculated by a resampling analysis. The graphical organization was referenced to the

1064 previous publication by Carey, *et al*[8].

1065

1066 **Fig. 5 Preferential genetic requirements for gluconeogenesis in the clinical *M.***

1067 ***intracellulare* strains inferred from the TnSeq results. a** Carbohydrate pathway

1068 showing the changes in Tn insertion reads. Genes identified with the resampling

1069 analysis are framed by squares. The essentiality of gluconeogenesis-related genes (*pckA,*

1070 *glpX*) was higher and that of glycolysis-related genes (*aceE, lpdC*) was lower in the

1071 clinical *M. intracellulare* strains compared with those in ATCC13950. **b** Data on genetic

1072 requirements calculated with a resampling analysis in the clinical *M. intracellulare*

1073 strains compared with ATCC13950. Red indicates a reduction in Tn insertion reads in

1074 the clinical *M. intracellulare* strains. Blue indicates an increase of Tn insertion reads in

1075 the clinical *M. intracellulare* strains. Asterisks indicate statistical significance of $\log_2$

1076 fold changes ($\log_2$FCs). The graphical organization was referenced to the previous

1077 publication by Carey, *et al*[8].

1078

1079 **Fig. 6 Detection of genes required for mouse lung infection in the clinical *M.***

1080 ***intracellulare* strains. a** Consistency between the genes required for infection in mouse

1081 lungs and the 175 genes required for hypoxic pellicle formation in ATCC13950. **b**

1082 Changes in the requirements for genes with increased genetic requirements observed in
1083 the clinical *M. intracellulare* strains after the infection of mouse lungs. Highlighted
1084 genes are also required for hypoxic pellicle formation by ATCC13950.
1085 Genetic requirements of the strain itself: genetic requirements compared with that of
1086 ATCC13950. Genetic requirements in mouse lungs: changes in the genetic requirements
1087 in the infected mouse lungs compared with those before infection. Gene set enrichment
1088 analysis: The genes listed as core enrichment are shown as "Yes" and the genes not
1089 listed as core enrichment are shown as "No."
1090
1091 **Fig. 7 Evaluation of the effect of the suppression of TnSeq-hit genes on the**
1092 **bacterial growth using the CRISPR-i system.** Open bar: day 3; closed bar: day 7. **a**
1093 Comparative growth rates of the knockdown strains relative to those of the vector
1094 control strains in the representative universal essential or growth-defect-associated
1095 genes: *glcB, inhA*, *gyrB* and *embB*. **b** Comparative growth rates of the knockdown
1096 strains relative to those of the vector control strains in the representative accessory and
1097 strain-dependent essential or growth-defect-associated genes: *pckA*, *glpX*, *csd* and ESX-
1098 5 type VII secretion components. Data are shown as the means ± SD of triplicate

1099 experiments. Data from one experiment representative of two independent experiments

1100 ($N = 2$) are shown.

1101

1102 **Fig. 8 Comparison of the timing of entry into logarithmic growth and logarithmic**

1103 **growth rate by the clinical *M. intracellulare* strains and ATCC13950. a**

1104 Representative data on the growth curves of each strain under aerobic and 5% oxygen

1105 conditions. The assay was performed three times in 96-well plates containing 250 μl of

1106 broth medium per well, in triplicate. Data are represented as CFUs in 4 μl sample at

1107 each timepoint. Data on the growth curves are the means of three biological replicates

1108 from one experiment. Data from one experiment representative of three independent

1109 experiments ($N = 3$) are shown. **b** Time at the inflection point (midpoint) on the sigmoid

1110 growth curve. *significantly earlier than an aerobic culture of ATCC13950;

1111 #significantly earlier than a hypoxic culture of ATCC13950; †significantly later than an

1112 aerobic culture of ATCC13950; ‡significantly later than a hypoxic culture of

1113 ATCC13950. **c** Growth rate at midpoint of the growth curve in each strain.

1114 #significantly slower than a hypoxic culture of ATCC13950; †significantly slower than

1115 an aerobic culture of the corresponding strain; ‡significantly faster than an aerobic

1116 culture of ATCC13950. Open bars: aerobic; closed bars: 5% O_2. Data are shown as the

means ± SD of triplicate experiments. Data from one experiment representative of three independent experiments ($N = 3$) are shown.

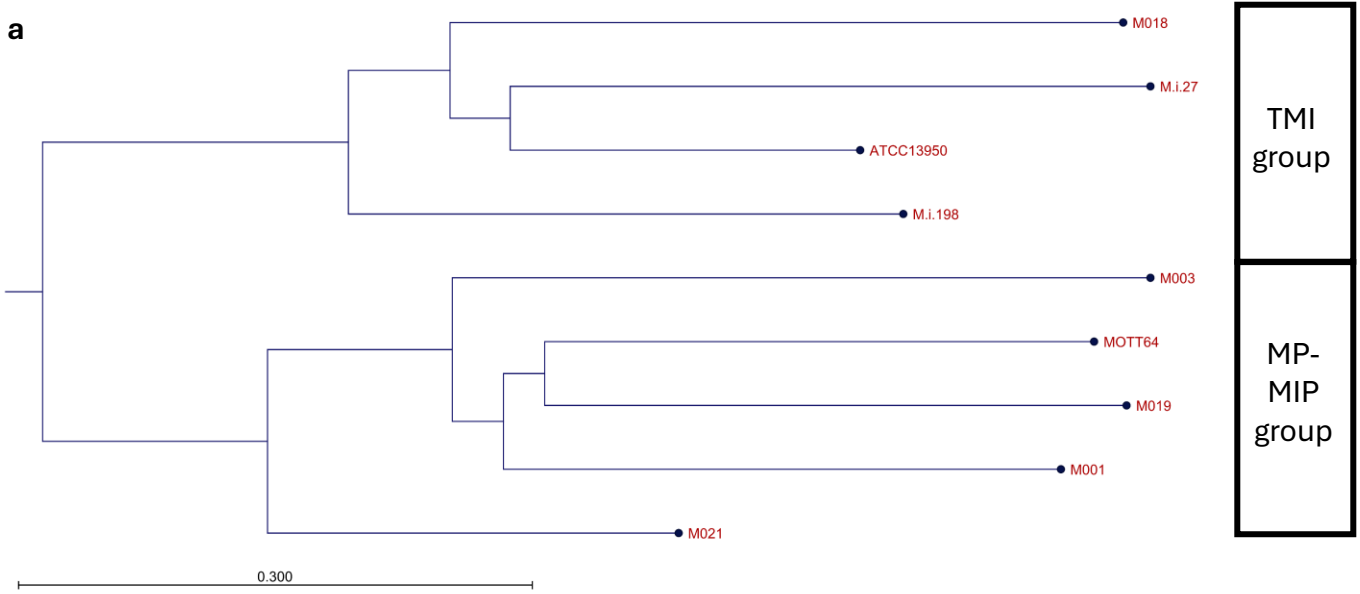
a
M018
M.i.27
ATCC13950
M.i.198
M003
MOTT64
M019
M001
M021
0.300
TMI group
MP-MIP group

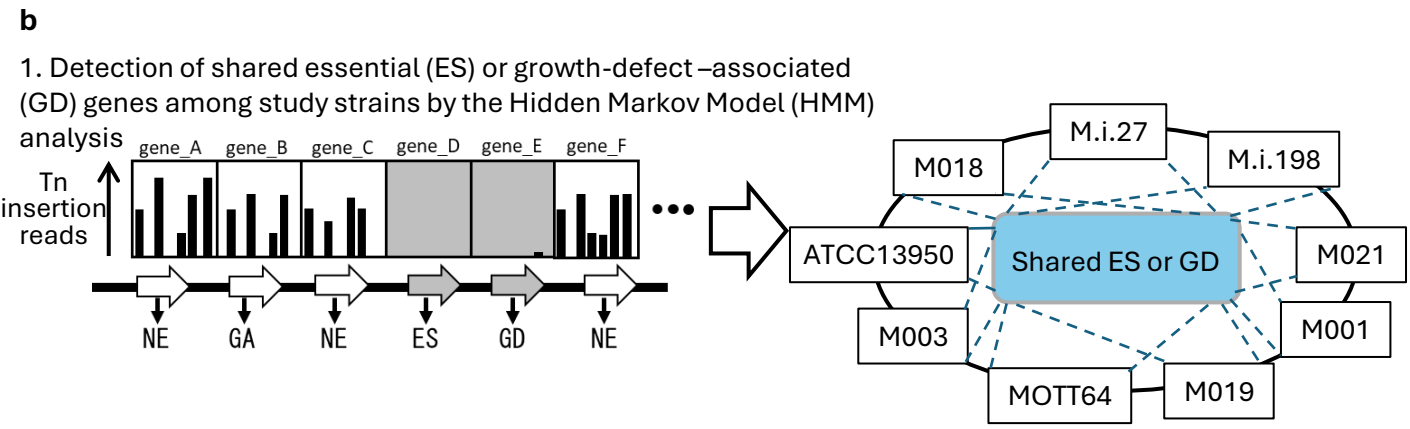
b
1. Detection of shared essential (ES) or growth-defect –associated (GD) genes among study strains by the Hidden Markov Model (HMM) analysis
gene_A
gene_B
gene_C
gene_D
gene_E
gene_F
Tn insertion reads
NE
GA
NE
ES
GD
NE
M.i.27
M018
M.i.198
ATCC13950
Shared ES or GD
M021
M003
M001
MOTT64
M019

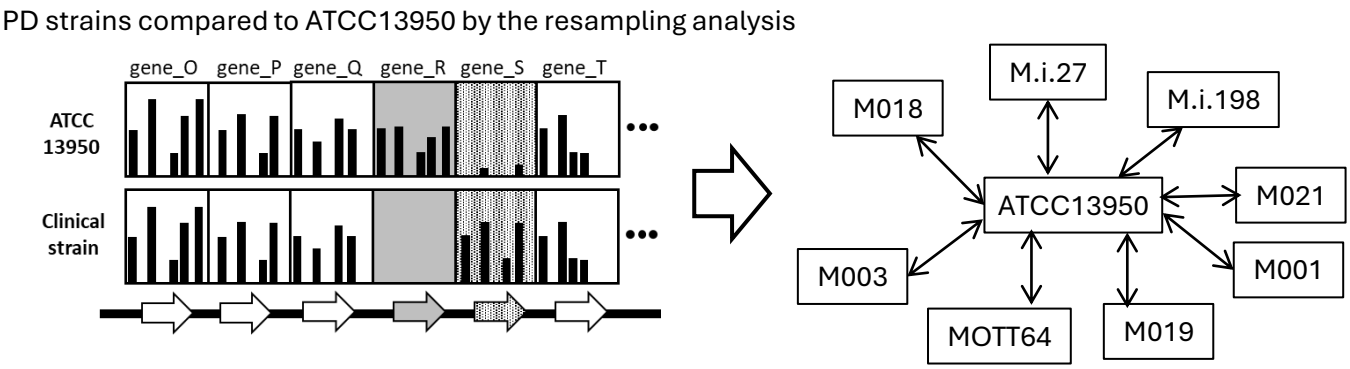
2. Detection of altered genetic requirements in clinical MAC-PD strains compared to ATCC13950 by the resampling analysis
gene_O
gene_P
gene_Q
gene_R
gene_S
gene_T
ATCC 13950
Clinical strain
M.i.27
M018
M.i.198
ATCC13950
M021
M003
M001
MOTT64
M019

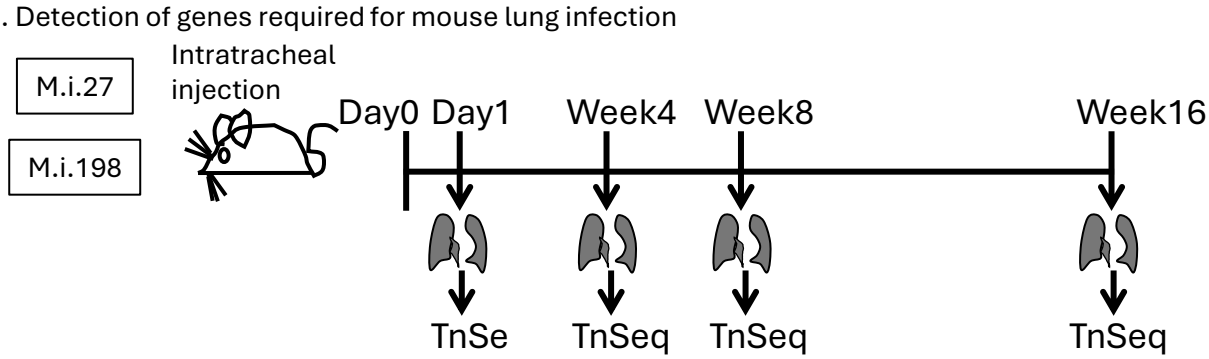
3. Detection of genes required for mouse lung infection
M.i.27
M.i.198
Intratracheal injection
Day0
Day1
Week4
Week8
Week16
TnSe
TnSeq
TnSeq
TnSeq

a

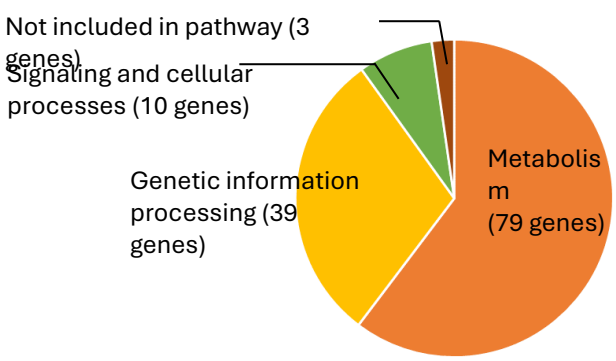

Metabolism: glyoxylate, purine/pyrimidine, amino acid, lipid, arabinogalactan/peptidoglycan, porphyrin

Genetic information processing: DNA replication, transcription, amino acid tRNA ligases, ribosomal proteins, general Sec proteins

Signaling and cellular processes: ABC transporter, type VII secretion system, iron-sulfur cluster assembly

Not Included in Pathway: hypothetical proteins

b

Gene locus	gene	function	target drug
OCU_RS25020, OCU_RS25025	*gyrB, gyrA*	DNA topoisomerase subunit B, intein-containing DNA gyrase subunit A	fluoroquinolones
OCU_RS26150	*embB*	arabinosyltransferase	ethambutol
OCU_RS40185	*inhA*	enoyl[acyl-carrier-protein] reductase FabI	isoniazid/ethionamid
OCU_RS45570	*alr*	alanine racemase	cycloserine
OCU_RS46225	*rpoC*	DNA-directed RNA polymerase subunit beta'	rifampicin
OCU_RS38100	*glcB*	malate synthase G	malate synthase inhibitors
OCU_RS32840, OCU_RS32845, OCU_RS32850	*atpA, atpG, atpB*	F_0F_1 ATP synthase subunit alpha, gamma, beta	bedaquiline

c

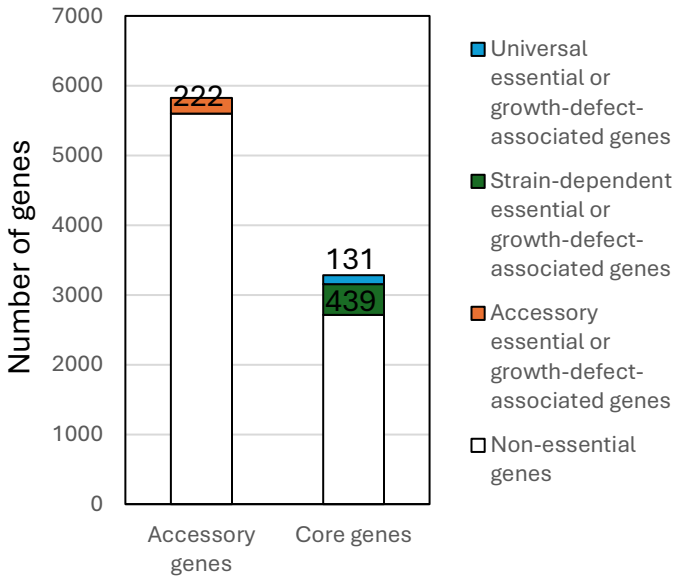

Fig. 2

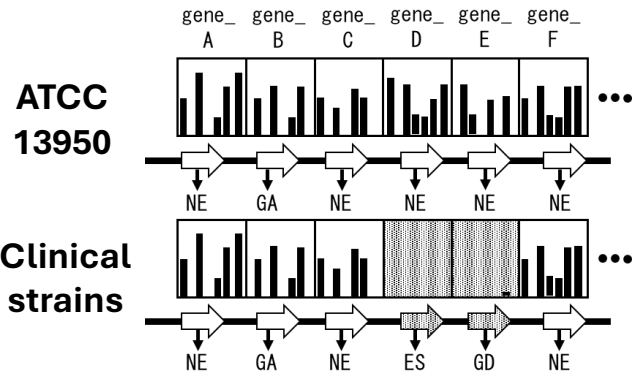

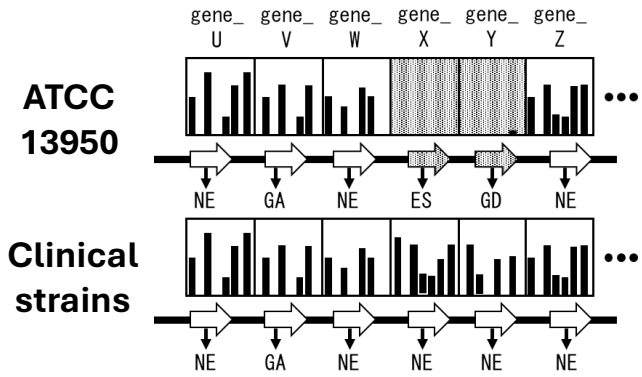

Tn decrease in clinical strains

A total of 121 genes were detected as significantly reduced Tn in clinical MAC-PD strains compared to ATCC13950. Of those, 9 genes were commonly hit in 3 to 5 clinical strains.

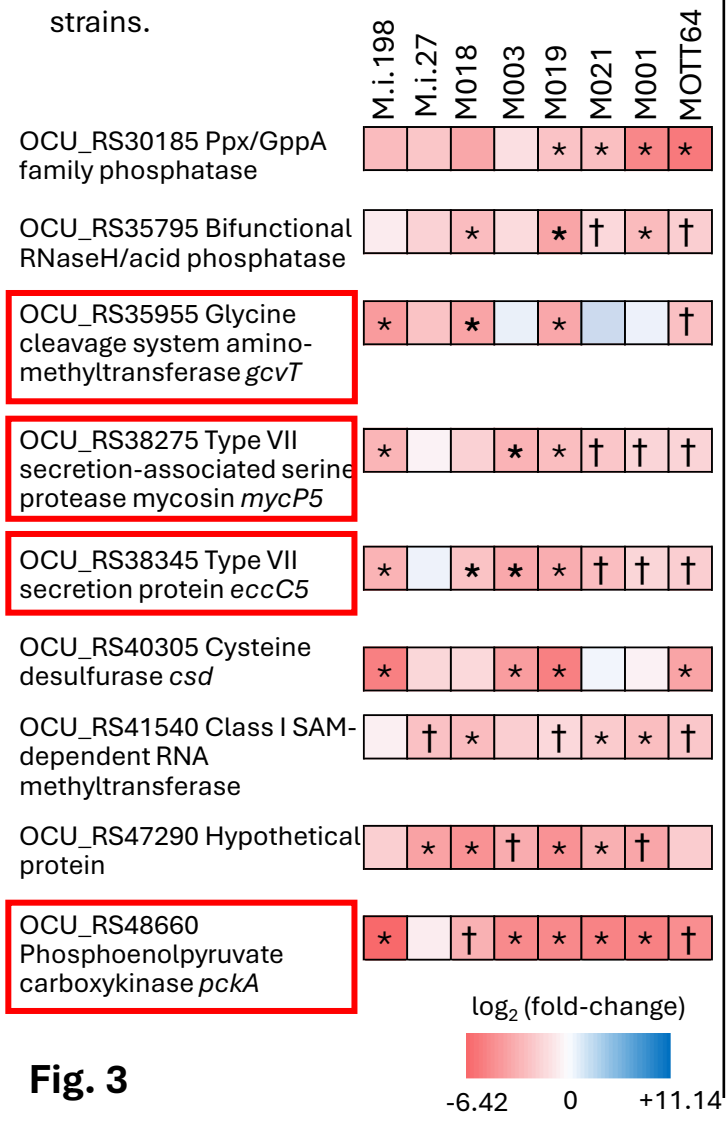

Tn increase in clinical strains

A total of 162 genes were detected as significantly increased Tn insertion compared to ATCC13950. Of those, 12 genes were commonly hit in more than 7 clinical MAC-PD strains.

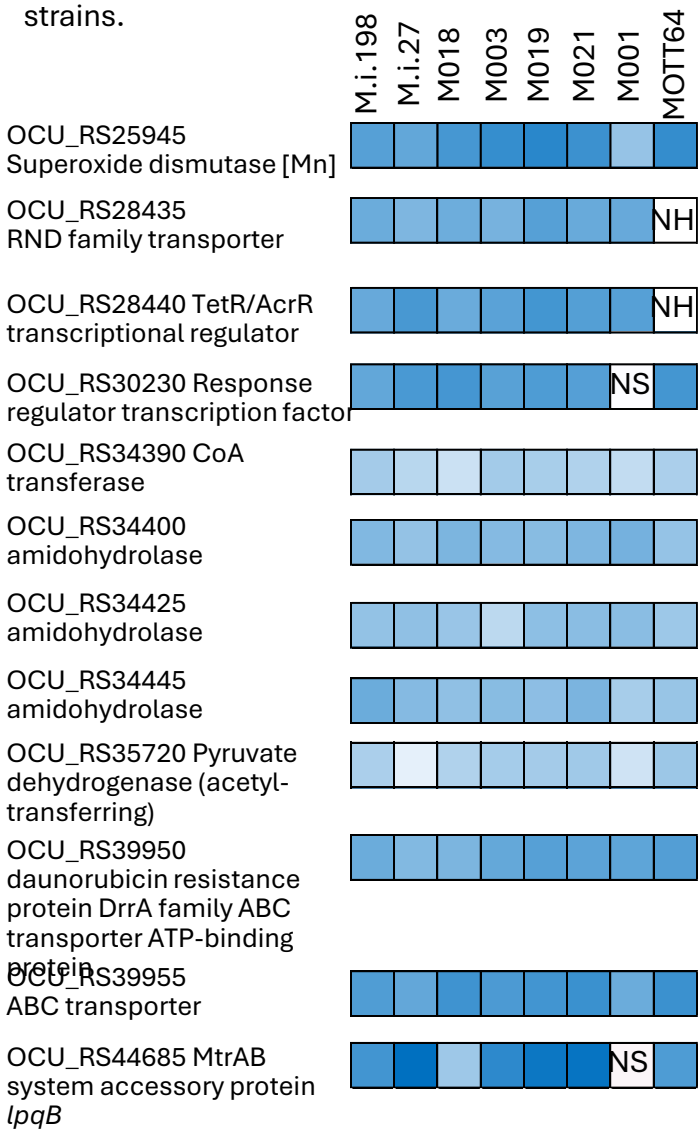

Fig. 3

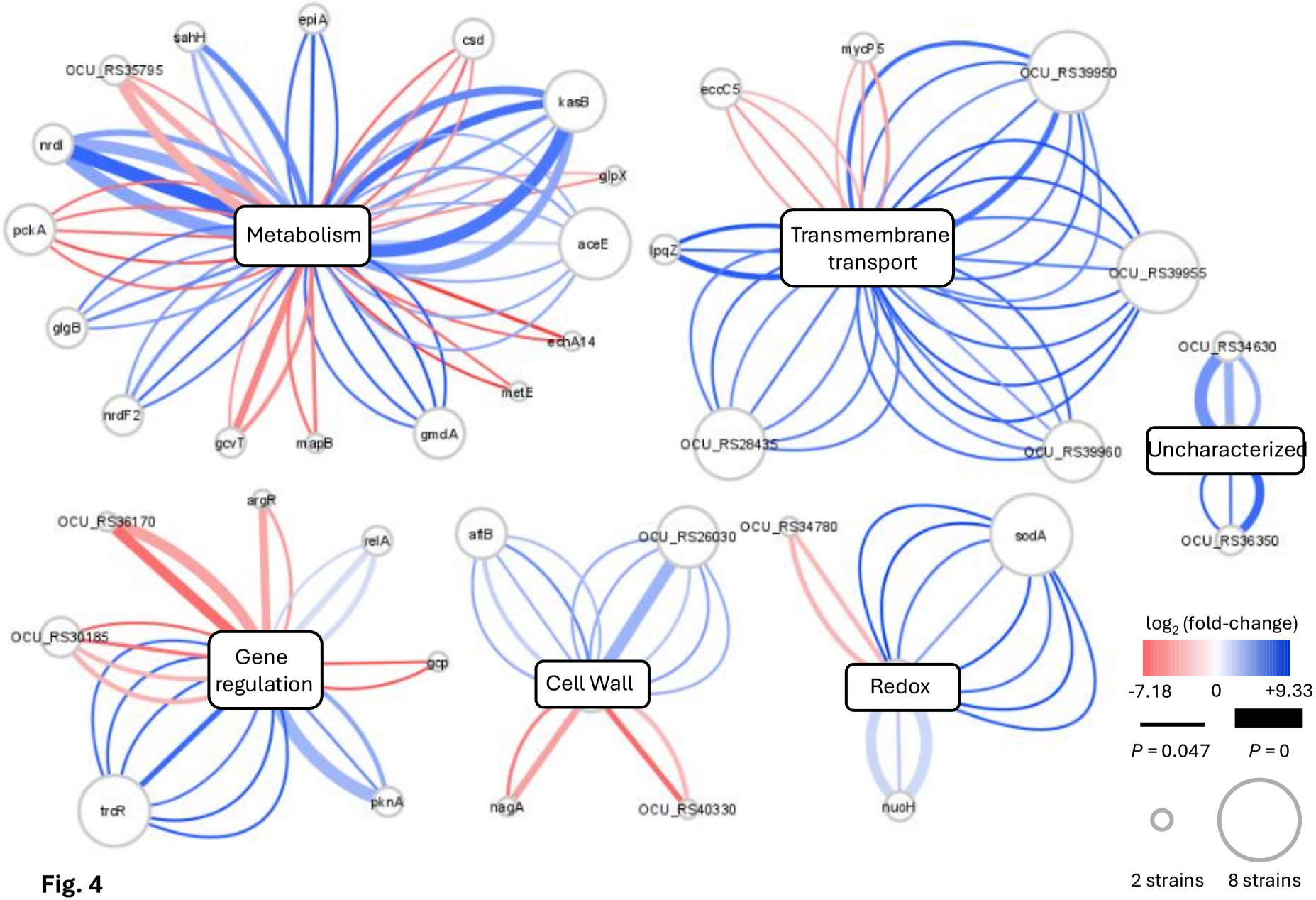
Metabolism
epiA
sahH
csd
OCU_RS35795
kasB
nrdI
glpX
pckA
aceE
glgB
echA14
metE
nrdF2
gcvT
mapB
gmdA
Transmembrane transport
mycP5
OCU_RS39950
eccC5
lpqZ
OCU_RS39955
OCU_RS28435
OCU_RS39960
Uncharacterized
OCU_RS34630
OCU_RS36350
Gene regulation
argR
OCU_RS36170
relA
OCU_RS30185
gcp
trcR
pknA
Cell Wall
atfB
OCU_RS26030
nagA
OCU_RS40330
Redox
OCU_RS34780
sodA
nuoH
log2 (fold-change)
-7.18
0
+9.33
P = 0.047
P = 0
2 strains
8 strains

Fig. 4

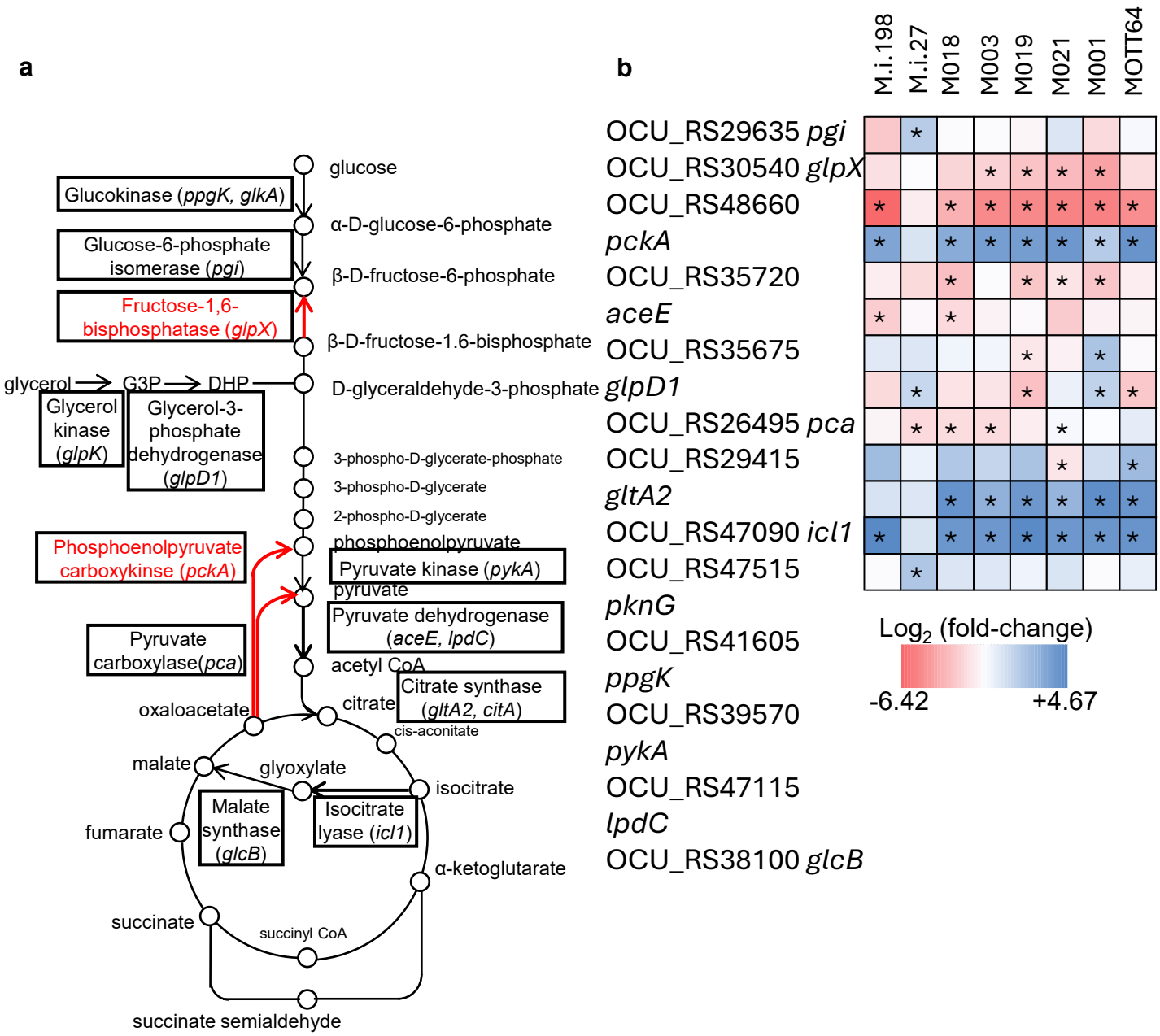
a
glucose
Glucokinase (ppgK, glkA)
α-D-glucose-6-phosphate
Glucose-6-phosphate isomerase (pgi)
β-D-fructose-6-phosphate
Fructose-1,6-bisphosphatase (glpX)
β-D-fructose-1.6-bisphosphate
glycerol
G3P
DHP
D-glyceraldehyde-3-phosphate
Glycerol kinase (glpK)
Glycerol-3-phosphate dehydrogenase (glpD1)
3-phospho-D-glycerate-phosphate
3-phospho-D-glycerate
2-phospho-D-glycerate
phosphoenolpyruvate
Phosphoenolpyruvate carboxykinse (pckA)
Pyruvate kinase (pykA)
pyruvate
Pyruvate dehydrogenase (aceE, lpdC)
Pyruvate carboxylase(pca)
acetyl CoA
Citrate synthase (gltA2, citA)
oxaloacetate
citrate
cis-aconitate
malate
glyoxylate
isocitrate
Malate synthase (glcB)
Isocitrate lyase (icl1)
fumarate
α-ketoglutarate
succinate
succinyl CoA
succinate semialdehyde
b
M.i.198
M.i.27
M018
M003
M019
M021
M001
MOTT64
OCU_RS29635 pgi
OCU_RS30540 glpX
OCU_RS48660
pckA
OCU_RS35720
aceE
OCU_RS35675
glpD1
OCU_RS26495 pca
OCU_RS29415
gltA2
OCU_RS47090 icl1
OCU_RS47515
pknG
OCU_RS41605
ppgK
OCU_RS39570
pykA
OCU_RS47115
lpdC
OCU_RS38100 glcB
Log2 (fold-change)
-6.42
+4.67

Fig 5.

a

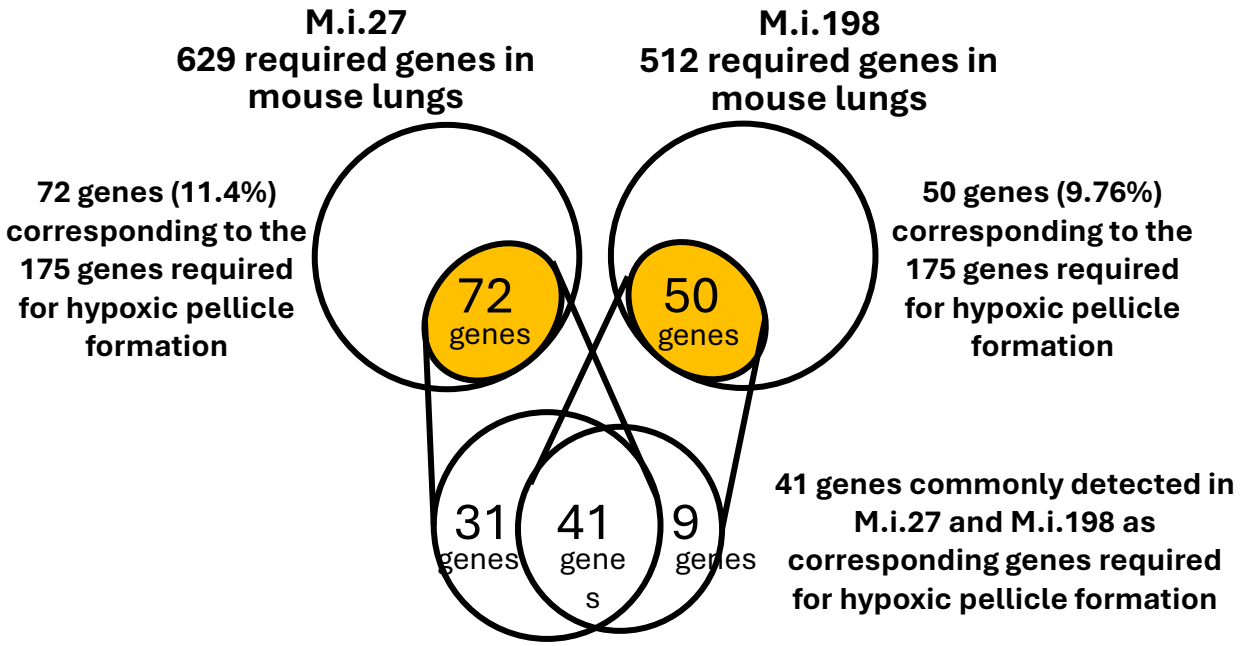

b

Locus_tag	Gene annotation	M.i.27 Genetic require-ments of strain itself	M.i.27 Genetic require-ments in mouse lungs	M.i.27 Gene set enrichi-ment analysis	M.i.198 Genetic require-ments of strain itself	M.i.198 Genetic require-ments in mouse lungs	M.i.198 Gene set enrichi-ment analysis
OCU_RS48660	Phoshoenolpyruvate carboxykinase PckA	NC	UP	Yes	UP	NC	No
OCU_RS30540	Fructose-1,6-bisphosphatase GlpX	NC	UP	Yes	NC	NC	Yes
OCU_RS40305	Cysteine desulfurase Csd	NC	UP	Yes	UP	NC	No
OCU_RS38345	TypeVII secretion protein EccC5	NC	UP	Yes	UP	NC	Yes
OCU_RS38275	TypeVII serine protease MycP5	NC	UP	Yes	UP	NC	No
OCU_RS35955	Glycine cleavage system aminomethyltransferase GcvT	NC	UP	Yes	UP	NC	Yes
OCU_RS30185	Ppx/GppA family phosphatase	NC	NC	Yes	NC	NC	Yes
OCU_RS35795	Bifunctional RNaseH/acid phosphatase	NC	NC	No	NC	NC	Yes
OCU_RS41540	Class I SAM-dependent RNA methyltransferase	UP	NC	No	NC	UP	Yes
OCU_RS47290	Hypothetical protein	UP	NC	Yes	NC	NC	Yes

Fig. 6

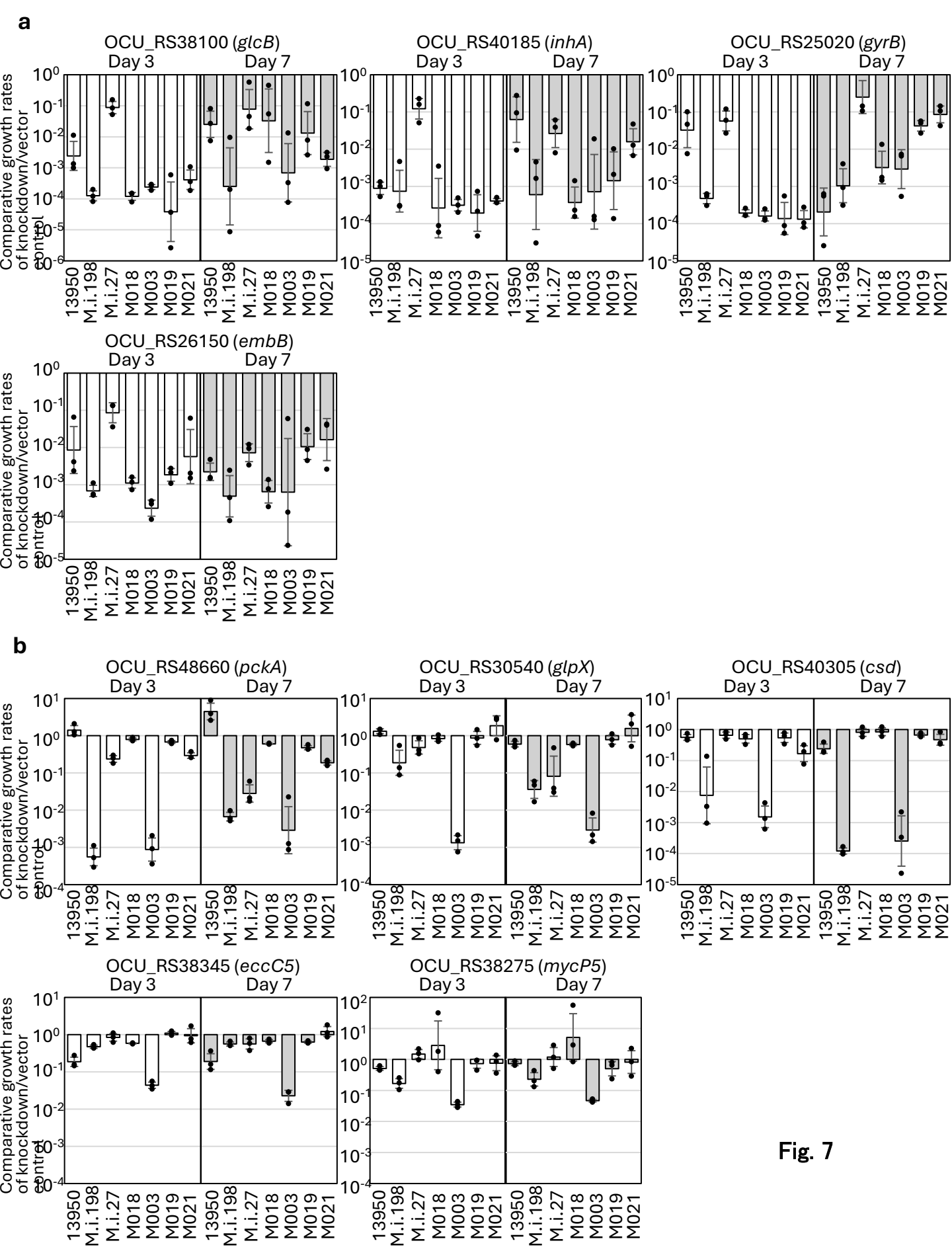
a
OCU_RS38100 (glcB)
OCU_RS40185 (inhA)
OCU_RS25020 (gyrB)
OCU_RS26150 (embB)
Day 3
Day 7
Comparative growth rates of knockdown/vector control
13950
M.i.198
M.i.27
M018
M003
M019
M021
b
OCU_RS48660 (pckA)
OCU_RS30540 (glpX)
OCU_RS40305 (csd)
OCU_RS38345 (eccC5)
OCU_RS38275 (mycP5)

Fig. 7

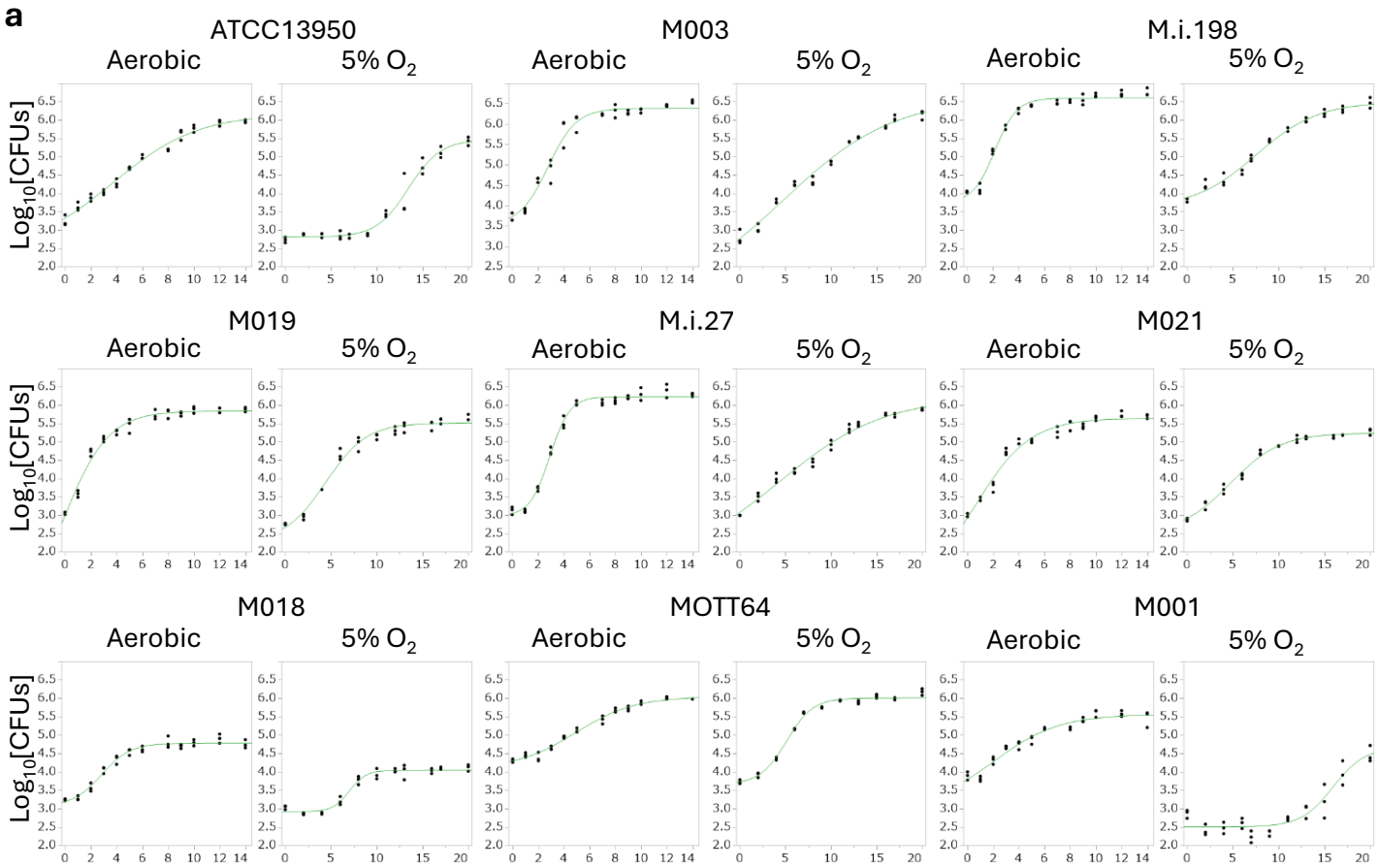
a
ATCC13950
M003
M.i.198
M019
M.i.27
M021
M018
MOTT64
M001
Aerobic
5% O2
Log10[CFUs]

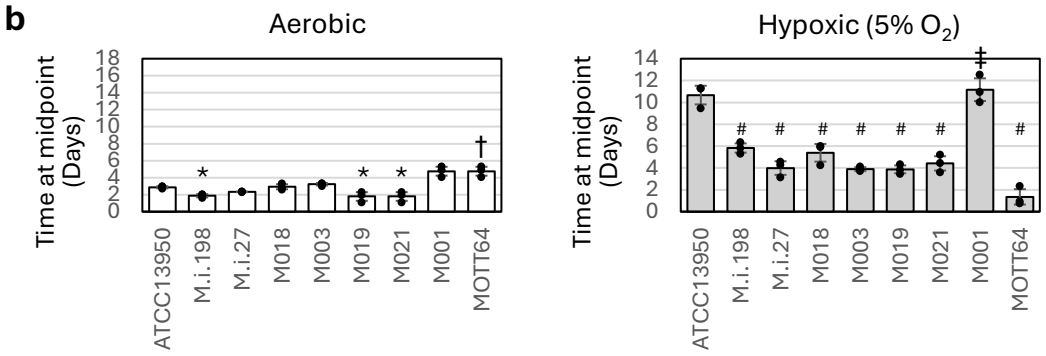
b
Aerobic
Hypoxic (5% O2)
Time at midpoint (Days)
ATCC13950
M.i.198
M.i.27
M018
M003
M019
M021
M001
MOTT64

Fig. 8

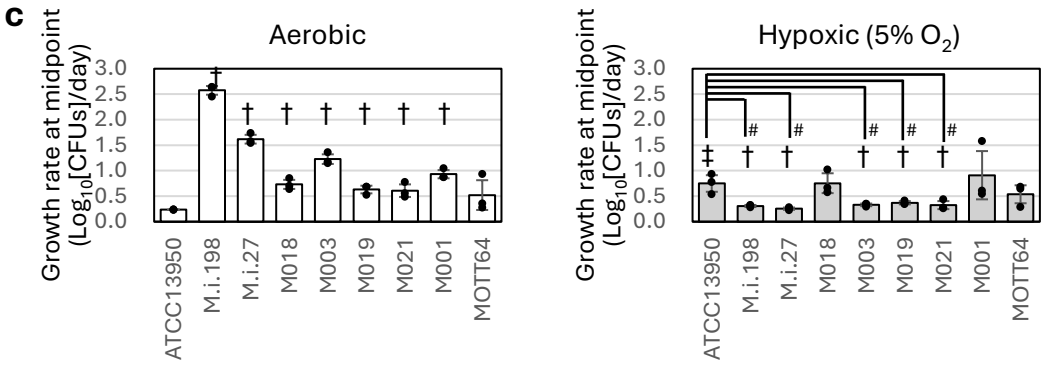
c
Aerobic
Hypoxic (5% O2)
Growth rate at midpoint (Log10[CFUs]/day)
ATCC13950
M.i.198
M.i.27
M018
M003
M019
M021
M001
MOTT64